Behnert, Marika; Bruckner, Thomas

Working Paper

Cost effects of energy system stability and flexibility options: An integrated optimal power flow modeling approach

Working Paper, No. 155

Provided in Cooperation with:
University of Leipzig, Faculty of Economics and Management Science

Suggested Citation: Behnert, Marika; Bruckner, Thomas (2018) : Cost effects of energy system stability and flexibility options: An integrated optimal power flow modeling approach, Working Paper, No. 155, Universität Leipzig, Wirtschaftswissenschaftliche Fakultät, Leipzig

This Version is available at:
https://hdl.handle.net/10419/182538

UNIVERSITÄT
LEIPZIG

Wirtschaftswissenschaftliche
Fakultät
Faculty of Economics and
Management Science

Working Paper, No. 155

Marika Behnert / Thomas Bruckner

Cost effects of energy system stability and flexibility options – an integrated optimal power flow modeling approach

September 2018

ISSN 1437-9384

Cost effects of energy system stability and flexibility options – an integrated optimal power flow modeling approach

Marika Behnert and Thomas Bruckner*

University of Leipzig
Institute for Infrastructure and Resources Management
Grimmaische Straße 12 · D–04109 Leipzig
behnert@wifa.uni-leipzig.de

Abstract

In this paper, a spatio-temporally resolved energy system model within the security-constrained optimal power flow framework using the direct-current loadflow approximation is proposed and applied to a techno-economic case study. The objective of the mixed-integer linear optimization problem (MILP) is to minimize the system's total costs, where the unit commitment model is coupled to electricity network constraints implementing a rolling horizon framework. The variables and equations are portrayed followed by a comparative scenario analysis. Therein, systemic impacts by a variation of import and export costs, the storage units' flexibilities and costs as well as changed nodal renewable energy sources feed-in profiles or maintenance actions of lines and thermal units are studied. Moreover, it is possible to (de)install and rescale technologies or lines belonging to a specific underlying network topology. By this, effects on endogenous variables such as line and thermal units' active powers, temporal storage level patterns or voltage angles are investigated.

Keywords

direct-current load flow model · security-constrained unit commitment · mixed-integer linear programming · energy system model · storage facility optimization · grid stability

*The authors thank S. Graupner for valuable comments and fruitful mathematical discussions.

1 Introduction

A major challenge towards a sustainable energy transition is the unification of interdependent dimensions represented by both the energy policy target triangle and the triple bottom line [EC, SH]. Environmental, economic, supply security and social aspects are essential for a flexible and stable energy system (ES). Moreover, time scales covering seconds to decades, the integration of stakeholder interests and regulatory frameworks on different hierarchy levels define multi-objective ecological, economic and technical power system targets. On the one hand, an increased penetration of fluctuating renewable energy sources (RES) and an enhanced share of decentralized and coupled infrastructures gain more relevance in order to preserve grid stability on all voltage levels and to establish innovative power-to-X conversion technologies. On the other hand, the decommission of conventional power plants and regional load profiles accompanied by different electricity market products and designs is a predominant topic. Therefore, intense efforts in interdisciplinary research are necessary, particularly addressing accurate load flow estimations.

[Sch, Gr] review the applicability of popular techno-economic ES modeling approaches including the experiences of their implementations. Generally, optimal power flow (OPF) is used for decision making at any planning horizon in ES operation and control ranging from long-term transmission network capacity planning to minute-by-minute adjustment of real and reactive power dispatch. A defining feature of OPF is the presence of the power flow equations in the set of constraints. More precisely, OPF describes any problem which seeks to optimize the operation of a power system – specifically for the security-constrained unit commitment (SCUC) of the generation and transmission of electricity – subject to physical constraints[1] imposed by electrical laws and engineering limits on the decision variables. The objective is to minimize the system's total cost of electricity generation while maintaining the ES within safe operating limits. Basic modeling constituents are the set of branches connected by a set of buses with controllable generators and loads located at specific nodes depending on a concrete grid topology. In addition to the unit commitment (UC), where physically limited scheduled thermal units are characterized by their on- and off-status or time-dependent output powers, SCUC takes into account line power flows. As an extension, SCUC ensures the physical realization of the optimal generation schedule produced by the UC algorithm in a power system by including network transmission constraints such as limited branch flow powers and bounded bus voltage deviations over multiple time periods. UC belongs to the class of complex large-scale, multi-period mixed-integer nonlinear (MINLP) optimization problems that are often linearized into MILP including binary decision variables. Due to the nonlinearity and non-convexity occuring in the constraints, quadratic costs or trigonometric functions originating from the exact alternating current load flow (ACLF) approach, sophisticated OPF approximation algorithms balancing convergence and accuracy were developed and tested [FR, W, B].

Concerning the modeling of network constraints, it is to check, whether the direct-current loadflow (DCLF) approximation for transmission systems is an appropriate choice for the considered ES. Under normal system operating conditions, the DCLF approach describes real power transfers quite accurately yielding rapid and robust, reliable and unique solutions, where the models are solved and optimized efficiently compared to the ACLF equations requiring iterative numerical methods due to their nonlinear

[1] In UC problems, one distinguishes global system constraints such as demand conservation or spinning reserve that are relevant for reliability and local, unit-specific or nodal constraints. They are valid for differently operating generator types (e.g. coal-fired, nuclear power plants or combined cycle gas turbines) with commitment schedules adhering to intertemporal parameters [T, W].

formulation and non-convexity [Sto]. For stressed systems revealing depressed voltages and large angle differences in emergency situations on long, heavily loaded transmission lines as well as for large voltage differences at distant nodes, the DC concept might evoke significant errors. Under normal operation, the assumption of a lossless transmission network can lead to deviating generator scheduling, different branch power flow or marginal fuel cost estimations. For this purpose, transmission loss approximations are sometimes respected in the DC framework [B, FR].

Following the derivation of the AC equations using line elements starting from equivalent circuits [ST, Bi], the nodal active and reactive contributions of the apparent power $S_k^{\mathrm{AC}} = P_k^{\mathrm{AC}} + jQ_k^{\mathrm{AC}}$ in the complex representation with the imaginary unit $j = \sqrt{-1}$ and a line km joining the buses k and m of a network reads[2]

$$\begin{aligned} P_k^{\mathrm{AC}} &= \sum_{km} \Big\{ |U_k|_{km}^2 \, g_{km} - |U_k| \, |U_m| \, g_{km} \cos\theta_{km} - |U_k| \, |U_m| \, b_{km} \sin\theta_{km} \Big\} \\ Q_k^{\mathrm{AC}} &= \sum_{km} \Big\{ - |U_k|_{km}^2 \, b_{km} + |U_k| \, |U_m| \, b_{km} \cos\theta_{km} - |U_k| \, |U_m| \, g_{km} \sin\theta_{km} \Big\} . \end{aligned}$$

A prominent example for the DC representation are high-voltage transmission lines carrying a high reactance compared to the resistive part of the line impedance $r_{km} \ll x_{km}$ yielding

$$(g_{km} + jb_{km}) = y_{km} = z_{km}^{-1} = (r_{km} + jx_{km})^{-1}$$

with a vanishing conductance $g_{km} \to 0$. Purely the susceptance b_{km} constitutes the admittance y_{km} leading to a reduced line impedance $z_{km}^{\mathrm{red}} = jx_{km}$. Rearranging $1 = j^2 b_{km} x_{km}$ gives $-b_{km} = \frac{1}{x_{km}}$. The mathematical assumptions for the simplified DC approach are the following. All branch resistances are approximately zero and the transmission system is assumed to be lossless. The stability criterion of small differences between adjacent voltage angles implies $\sin\theta_{km} \to \theta_{km}$ and $\cos\theta_{km} \to 1$. Reactive powers are neglected $Q_k^{\mathrm{AC}} \to 0$ and bus voltages are approximated by $|U_{k,m}| = 1$ per unit [Sch, Bi]. The result is the linearized DCLF expression

$$P_k^{\mathrm{DC}} = \sum_{km} x_{km}^{-1} (\theta_k - \theta_m) = \sum_{km} -b_{km} \theta_{km}.$$

In [N], different exemplary techno-economic ES modeling approaches considering grid constraints are presented focusing on capacity expansion planning. Using a linear DC OPF model, the development of the German power generation between 2007 and 2030, nodal prices and occuring bottlenecks for 2030 are analyzed, respectively. Moreover, an AC power flow model describing the distribution power grid employing the technical AC modeling software NEPLAN is developed in order to take into account backfeeding processes due to an increased electricity decentralization. Thereafter, an AC modeling approach is discussed additionally addressing economic effects. Considering an eleven-zone power system, a nodal pricing AC OPF calculation is performed by means of a total generation cost minimization in [Kr]. The author optimizes three cases by assuming different network topologies with the aim to investigate price areas as well as transmission congestion such that it can be applied to the Nordic market or by the Norwegian transmission system operator. In a case study for Germany in 2020, Eickmann et al. examine the interaction

[2] Appendix e provides a nomenclature of symbols in electrical engineering.

of storage operation and transmission grid congestion in order to evaluate the potential of a secure grid operation within a two-stage hourly resolved contingency analysis [Ei]. Therein, a security-constrained OPF model is set up to estimate the influence of storage expansion on the UC and the redispatch energy with its associated costs. Fu et al. study a six- and 118-bus system including thermal units and demands with AC constraints based on an iterative cost-minimal SCUC approach [F]. At first, the hourly UC is determined by solving a master problem neglecting security network constraints followed by rescheduled subproblems until network violations are eliminated and convergence is reached.

An appropriate approach in this paper is the choice of the SCUC-OPF framework applying the DCLF approximation within an MILP optimization. The research questions in this study address economic and technical scenarios compared to a benchmark with respect to nodal ES components by considering cross-border electricity exchange activities, the temporal charging behavior of storage facilities, the occurence of strong wind, a solar eclipse and planned line repair or power plant maintenance. The modifications of specific parameters like storage facility flexibilities and rescaled RES feed-in profiles are introduced in section 3. We study effects on the following endogenous time-dependent quantities, ceteris paribus (c.p.).

- Which sensitivity does the objective function, i.e. the ES *total costs*, with respect to altered scenario inputs show?
- How do *voltage angles* and *line active powers*[3] at the slack bus[4] or the RES feed-in nodes react?
- Which behavior is revealed by the *supplied power* and *commissioning state for each generator*?
- In which manner do *import* or *export* amounts change?
- We inspect charging patterns of *storage facilities* for varied costs and (dis)charging rates.
- The response to *line and power plant maintenance* during several hours on special days is examined.

The remainder of this work is organized as follows. In section 2, the mathematical design of a highly aggregated ES model equipped by a topology resembling the German transmission grid of 28 nodes and 45 lines is developed. Its input data and program description are documented in order to investigate techno-economic scenarios that deviate from a reference case. In section 3, the above research questions and the system cost sensitivities are assessed. Section 4 summarizes the main conclusions drawn and emphasizes future tasks. The appendix provides mathematical derivations and a nomenclature.

2 SCUC optimal power flow ES model description

In the following, we present the exogenous input time series, ES modeling equations and variables. Since dimensions are conserved, the model is formulated in arbitrary energy [e.u.] and monetary [m.u.] units.

[3] Reactive power contributions originating from the ACLF method are neglected. We only consider active powers P_k^{DC}.

[4] In load flow studies, the voltage magnitude and angle are fixed and the power injections are free at the chosen slack bus of the ES taken as reference [FR]. For a detailed description, see [SM], section 5.2.3.

2.1 Input data and network topology

Figure (1) depicts the input time series with a period index $t = \{0, ..., 24\}$ for an illustrative day. In the modeling equations, the elements of the set $days = \{1, 2, 3\}$ are joined by means of the rolling horizon concept, where the optimization runs over equidistant time steps encompassing three subsequent days with 24 hours. $NOL_{t,N}$ portray scaled standardized commercial G_0 or household H_0 hourly demand profiles located at a node N, where the aggregate time series is summed over all nodal loads $D_t = \sum_N NOL_{t,N}\ \forall t$. Moreover, positive and negative time-dependent reserve power contributions $\pm Res_t$ are taken into account. Typical feed-ins of photovoltaics $PV_{t,N}$, $wind_{t,N}$ and a pumped-storage hydro power plant time series $pshp_{t,N}$ are displayed in figure (1). According to our chosen sign convention, energy flows into the system, i.e., imports, thermal generation and RES feed-in, discharging or turbining processes are positive. Withdrawals such as loads, exports, charging or pumping have negative signs.

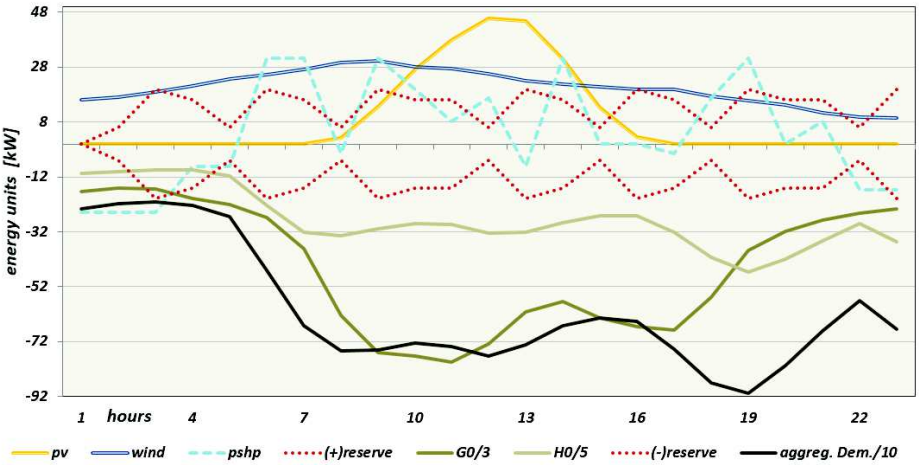

Figure 1: Diurnal standard load (G_0, H_0), cumulated scaled demand and spinning reserve energy profiles and nodal PV, wind and PSHP input time series.

Figure (2) illustrates a stylized grid topology consisting of 28 nodes designed by Handschin et al. [H]. At each node $N \in \mathcal{N} = \{N_1, ..., N_{28}\}$, loads, generators, storage, RES feed-in, import or export processes are installable ex-ante. The transmission lines $L_{N,NP} \in \mathcal{L} = \{L_1, ..., L_{45}\}$ connecting two buses $N \neq NP$ specify the grid topology. The technical network data table $LD_{N,NP}$ comprises the susceptance $B_{N,NP}$ normalized by line lengths, the length of each line, its capacity power limit and number of wires. Figure (2) shows that a line carries up to six parallel wires. It is derived in appendix a that parallel susceptances add up. To comply with the (N-1)-criterion[5], at least two adjacent systems are set up. Figure (2) visualizes that processes might occur simultaneously at one topological bus guaranteeing the integration of multiple nodal flexibility options. For example, at N10, load is demanded, PV and two fossil-fueled generators are installed. Another example is the cross-border interconnector bus N5 with nodal demand, wind generation and a (dis)chargeable energy storage facility.

[5]"the system is planned such that, with all transmission facilities in service, the system is in a secure state, and for any one credible contingency event, the system moves to a satisfactory state. However, if more than one contingency event was to occur, load may have to be shed to return to a satisfactory state" [EA]. "A *contingency* is defined as an event which removes one or more generators or transmission lines from the power system, increasing the stress on the remaining network" [FR].
Besides the deterministic (N-1) principle, probabilistic reliability criteria account for RES feed-in uncertainties [O].

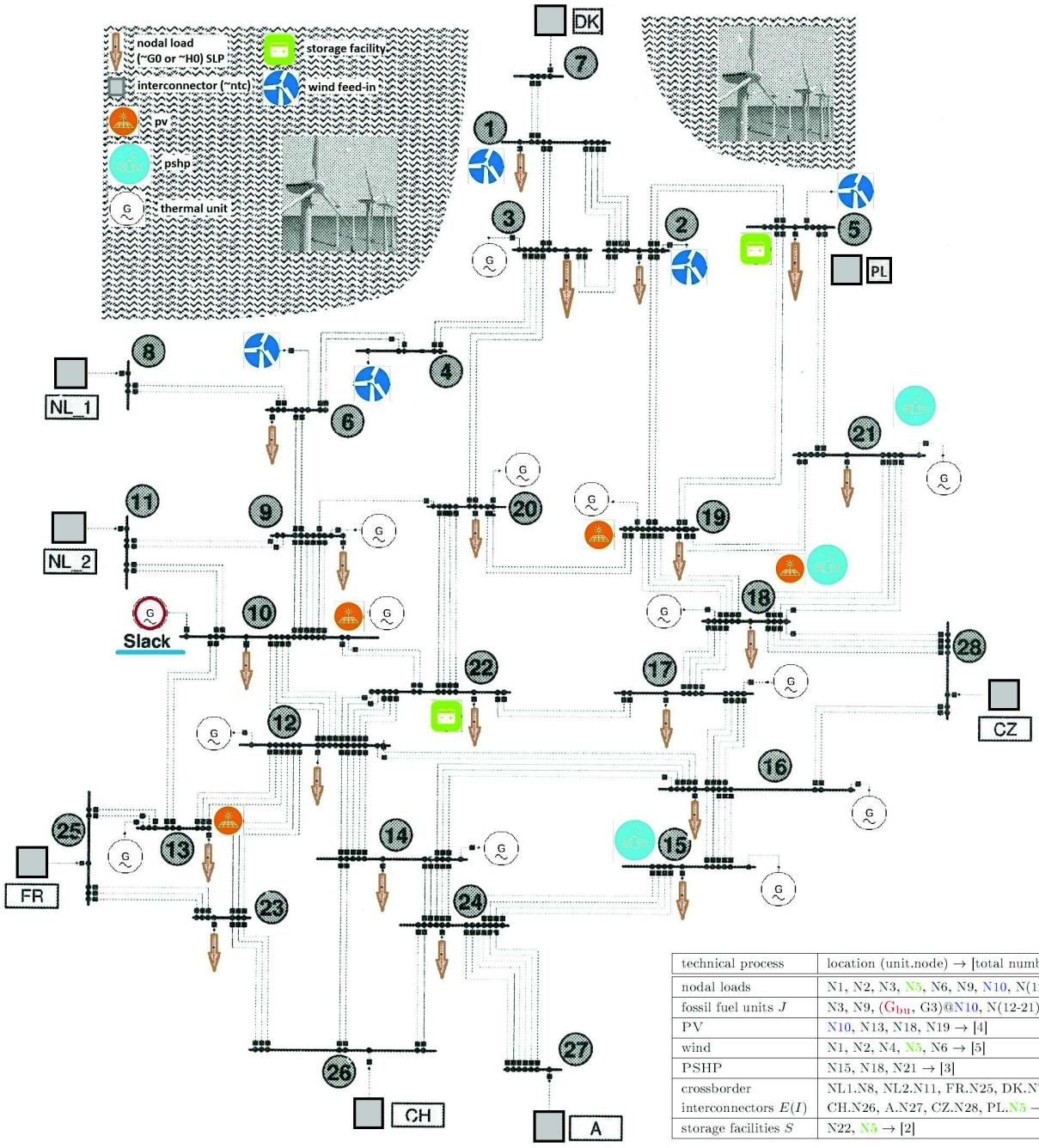

technical process	location (unit.node) → [total number of nodes]
nodal loads	N1, N2, N3, N5, N6, N9, N10, N(12-24) → [20]
fossil fuel units J	N3, N9, (G_{bu}, G3)@N10, N(12-21) → [14]
PV	N10, N13, N18, N19 → [4]
wind	N1, N2, N4, N5, N6 → [5]
PSHP	N15, N18, N21 → [3]
crossborder interconnectors $E(I)$	NL1.N8, NL2.N11, FR.N25, DK.N7, CH.N26, A.N27, CZ.N28, PL.N5 → [8]
storage facilities S	N22, N5 → [2]

Figure 2: Aggregated ES model topology resembling the German electricity transmission system with lines equipped by different numbers of wires and lengths based on [H]. The nodal-assigned technologies, import and export buses (gray squares), RES feed-in, storage facilities, PSHP as well as thermal units (icons, top left) and loads (brown arrows) are listed in the table above.

Fossil-fueled generators are labeled by $j \in \mathcal{J} = \{G_1, ..., G_{13}, G_{\mathrm{bu}}\}$, where a flexible, expensive back-up power plant G_{bu} takes a stabilizing function. In figure (4), generators are characterized by minimal and maximal active powers $P_j^{\min}$ and $P_j^{\max}$, respectively[6]. Ramp rates describe the gradients of operational flexibility. Moreover, fixed, start-up, shut-down cost contributions and variable costs per output power

[6] An intermediate value P^a creates partial slopes accounting for the piecewise linearized quadratic generation cost function sketched in figure (3, left).

are given.

Imports and exports with net transfer capacities, fixed costs c^f_{Im} and c^f_{Ex} accounting for the interconnector installation and variable revenues (costs) c^v_{Ex} and c^v_{Im} denote the power delivered (imported) at the cross-border interconnectors with scaled maximum transport values based on [R].

In the model, dynamically chargeable electricity storage facilities $s \in \mathcal{S} = \{S_1, S_2\}$ are confined by capacity limits $c^{\min}_s$ and $c^{\max}_s$. The amount of possible level changes between two consecutive hours is parametrized via the upper (lower) discharging and charging gradients. Besides, storage technologies are marked by fixed installation c^f_s and variable discharging and charging costs c^v_{dis} and c^v_{ch}, respectively.

2.2 Mathematical formulation of the model

This subsection includes parameters, variables, and equations implemented in the GAMS program code.

The compact structure of an OPF problem [B, FR] is given by

$$
\begin{array}{lcl}
 & \min_{\phi} goal(\phi) & \\
\text{subject to} & & \\
g(\phi) & = & 0 \text{ (equality constraints)} \\
h(\phi) & \leq & 0 \text{ (inequality constraints)} \\
\phi^{\min} & \leq \phi \leq & \phi^{\max} \text{ variables characterizing the feasible set.}
\end{array}
$$

With regards to numerical parameters, an average price was set for PSHP generation. The marginal cost of solar and wind feed-in are zero corresponding to RES subsidy schemes similar to the governmental support like the German EEG law.

Besides the objective function to be minimized – the system's total costs *goal* – these time-dependent *positive* endogenous variables are defined:

- import, export $p_{\mathrm{Im},t}$, $p_{\mathrm{Ex},t}$ and output powers $p_{j,t}$ for the generator j in period t,
- shut-down $C^{\mathrm{sd}}_{j,t}$ and stairwise approximated start-up $C^{\mathrm{st}}_{j,t}$ costs of thermal units,
- $\lambda_{i,j,t}$ auxiliary segment variable to linearize the production costs,
- storage state $ch_{s,t}$, discharging and charging amounts $qq_{s,t}$ and $q_{s,t}$ as well as discharging and charging rates $disch_{s,t}$ and $charge_{s,t}$, respectively.

Positive and negative values are possible for the following variables.

- $C^{\mathrm{fuel}}_{j,t}$ and $y^{\mathrm{em}}_{j,t}$ are related to the piecewise linearized production costs and emission functions.
- $cc_{s,t}$ denotes an auxiliary charging variable for a storage facility s.
- $da_{N,t}$ is the voltage angle at the node N with a difference $\theta_{N,NP,t} = da_{N,t} - da_{NP,t}$ between two connected nodes $N \neq NP$.
- $LPOW_{L,t}$ represents the power time series transmitted over a line $L_{N,NP}$.

Binary variables with the values of 0 and 1 describe the on- and off- state of a technical process,

- $v_{j,t} = 1$ thermal unit j committed in t,
- $y_{j,t} = 1$ thermal unit j started up at the beginning of t,
- $z_{j,t} = 1$ thermal unit j shut down at the beginning of t,
- $bin_{i,j,t}$ auxiliary segment variable to linearize the production costs,
- $v_{\mathrm{Im},t} = 1$ and $v_{\mathrm{Ex},t} = 1$ import and export committed in t,
- $a_{s,t} = 1$ and $b_{s,t} = 1$ charging and discharging committed in period t.

To overcome nonlinearities, we define auxiliary parameters. Linearization methods are applied to the power plant start-up, emission and production costs, as sketched in figure (3). In scheduling problems, assuming quadratic generation fuel cost functions is common [SM, Ta],

$$C_j^{\mathrm{prod}} = f_j(p_{j,t}) = (\delta_j + \epsilon_j p_{j,t} + \kappa_j p_{j,t}^2) \text{ with coefficients } \{\delta, \epsilon, \kappa\}_j .$$

Therein, $p_{j,t}$ denotes the time-dependent power supply of a fossil-fueled power plant j. The task is to minimize a separable function by considering it as the sum of functions of a scalar variable $p_{j,t}$ such that nonlinear terms are approximated piecewise with the aim to obtain linear or integer programming models. Accuracy of the original equation is reached via enhancing the number of segments, see the mathematical derivation in appendix b and [P].

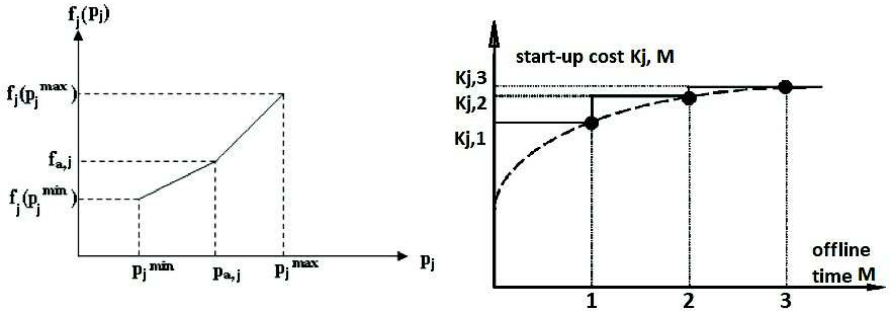

Figure 3: *left:* Approximation of quadratic fuel costs $C_j^{\mathrm{prod}} \approx C_{j,t}^{\mathrm{fuel}}$ using two linear segments [Ta]. *right:* Visualization of exponential, discrete and stairwise start-up cost functions [CA].

This procedure applies analogously to the linearization of the emission cost function of thermal units that consists of a quadratic and exponential contribution depending on $p_{j,t}$ [SM]. The ecological OPF problem seeks to minimize total emissions of CO_2, SO_2 and NO_x pollutants as a function of the generators' power,

$$\min \left\{ \sum_{j,t} E_j(p_{j,t}) \right\} \text{ with } E_j(p_{j,t}) = \left\{ \alpha_j + \beta_j \cdot p_{j,t} + \gamma_j \cdot p_{j,t}^2 \right\} \left[\tfrac{\mathrm{tons}}{\mathrm{hour}}\right] \text{ and the constants } \{\alpha, \beta, \gamma\}_j,$$

see appendix b.

Minimal up- and downtimes UT_j and DT_j and the time required to cool a unit down T_j^{cool} express that it cannot be turned on and off immediately. Accordingly, yG_j and zG_j accumulate the number of periods

a power plant underlies maximal daily switching-on and -off events. To approximate the production and emission functions, linearization intervals indicated by $i = \{1, 2, 3\}$ are provided.

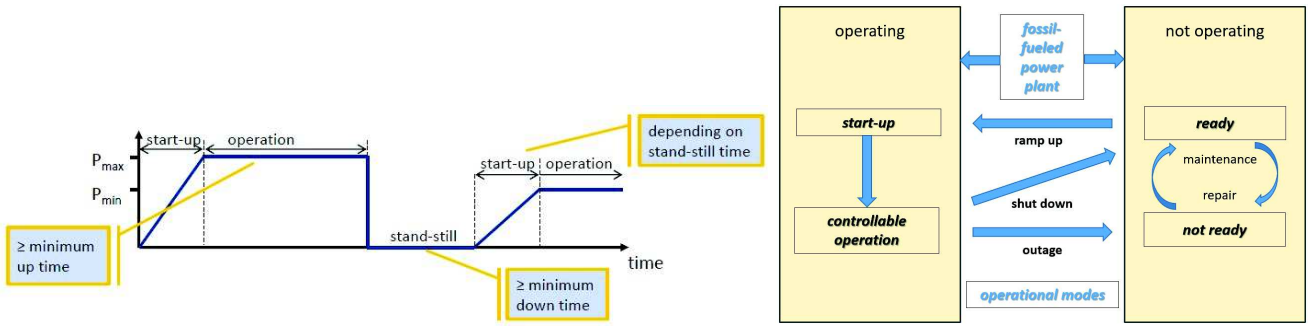

Figure 4: Operational constraints [D] and characteristic modes of fossil-fueled power plants based on [Ste].

Start-up costs are modeled stairwise instead of using a constant value. In a strict sense, they increase exponentially, as illustrated in figure (3, right) by

$$K^{\text{st}}_{j,M} = \Phi_j \cdot \left[1 - e^{-l \cdot M}\right] + F_j \text{ with the offline time counter } M \leq M^{\max} = \left[T^{\text{cool}} + DT\right]_j \text{ [hours]}.$$

For a complete cold start of unit j, they are the sum of the plant-specific variable and fixed costs $\Phi_j + F_j$ comprising time-independent contributions such as labor, wear and tear as well as a heat loss coefficient l. By means of a binary variable formulation, the start-up costs are expressed via the piecewise increasing step function

$$\widetilde{K^{\text{st}}_j} \geq K^{\text{st}}_{j,M^{\max}} \cdot \left\{ v_{j,t} - \sum_{M=1}^{M^{\max}} v_{j,t-M} \right\}, \tag{1}$$

see figure (3, right). $K^{\text{st}}_{j,M^{\max}}$ depends on a fixed number of maximal looking-back time steps $M^{\max}$ before a thermal unit starts up [Si, Bö].

In order to classify the modeling equations that are valid after the preplanning period $day = 1_{t \geq 1}$, we group four types to provide a comfortable overview.

a. system balance and goal function

The MILP objective function *goal* [m.u.] to be minimized depends linearly on the optimization variables. It is summed over all time steps t comprising several cost types. Quadratic or exponential terms are approximated and products of binary variables are linearized exploiting techniques documented in appendix b and c. Production costs C^{therm} and emission costs C^{em} depend on the delivered power $p_{j,t}$ of a generator in case it was committed. A synthetic time series p^{em}_t accounts for the fossil-fueled units' emission prices. Therefore, start-up and shut-down binary variables $\{v,\ y\ , z\}_{j,t} \in \{0, 1\}$ are used. In general, the feed-in powers of exogenous RES and PSHP are multiplied by the specific costs p^{PV}_t, p^{wind}_t and p^{PSHP}_t $\left[\frac{\text{m.u.}}{\text{e.u.}}\right]$ to obtain their associated costs. If import or excess power is required to cover the load, costs ${c^v}_{\text{Im}}$ or export revenues ${c^v}_{\text{Ex}}$ and fixed installation costs ${c^f}_{\text{Im,Ex}}$ emerge, respectively. Furthermore, fixed c^f_s and variable storage costs ${c^v}_{\text{ch},s}$ and ${c^v}_{\text{dis},s}$ are included. Based on [Bö], the objective reads

$$
\begin{aligned}
goal \;&:=\; \sum_{t} \left\{ C^{\text{therm}} + C^{\text{em}} + C^{\text{RES}} + C^{\text{PSHP}} + C^{\text{Im}} + C^{\text{Ex}} + C^{\text{store}} \right\} \\
&=\; \sum_{t,j} C^{\text{fuel}}_{j,t} + C^{\text{st}}{}_{j,t} + C^{\text{sd}}{}_{j,t} + p^{\text{em}}_{t} \cdot y^{\text{em}}_{j,t} \\
&+\; \sum_{t,N} PV_{t,N} \cdot p^{\text{PV}}_{t} + wind_{t,N} \cdot p^{\text{wind}}_{t} + pshp_{t,N} \cdot p^{\text{PSHP}}_{t} \\
&+\; \sum_{t,\text{Im}} \left[c^{f}_{\text{Im}} \cdot v_{\text{Im},t} + c^{v}_{\text{Im}} \cdot p_{\text{Im},t} \right] + \sum_{t,\text{Ex}} \left[c^{f}_{\text{Ex}} \cdot v_{\text{Ex},t} - c^{v}_{\text{Ex}} \cdot p_{\text{Ex},t} \right] \\
&+\; \sum_{t,s} \left[c^{f}_{s} + c^{v}{}_{\text{ch},s} \cdot q_{s,t} + c^{v}{}_{\text{dis},s} \cdot qq_{s,t} \right] .
\end{aligned} \tag{2}
$$

Following [T], the positive and negative spinning reserve constraints are

$$
\begin{aligned}
\textstyle\sum_N \left[PV_{t,N} + wind_{t,N} + pshp_{t,N} \right] + \sum_j P^{\max}_{j} \cdot v_{j,t} + \sum_s \;\; [qq_{t,s} - q_{t,s}] \geq D_t + Res_t \\
\textstyle\sum_N \left[PV_{t,N} + wind_{t,N} + pshp_{t,N} \right] + \sum_j P^{\min}_{j} \cdot v_{j,t} + \sum_s \;\; [qq_{t,s} - q_{t,s}] \leq D_t - Res_t .
\end{aligned}
$$

Referred to [CC], our adapted equality constraint balances the nodal energy contributions,

$$
\begin{aligned}
&\left\{ \sum_{j} p_{j,t} + \sum_{\text{Im}} p_{\text{Im},t} - \sum_{\text{Ex}} p_{\text{Ex},t} + \sum_{s} \left[qq_{s,t} - q_{s,t} \right] \right\}_{N=N^*} + \sum_{NP} \left\{ B_{N,NP} \cdot \theta_{N,NP,t} + B_{NP,N} \cdot \theta_{N,NP,t} \right\} \\
=\;& NOL_{t,N} - \left[PV_{t,N} + wind_{t,N} + pshp_{t,N} \right] \; \forall t \, \forall N \neq NP.
\end{aligned} \tag{3}
$$

In equation (3) above, thermal units $j \in \mathcal{J}$, storage $s \in \mathcal{S}$, import and export processes {Im, Ex} are mapped in the GAMS program code to their associated topological nodes $N^* \in \mathcal{N}$ according to figure (2) such that these are nodal expressions.

Import and export activities are limited via

$$
\begin{aligned}
P^{\min}_{\text{Im}} \cdot v_{\text{Im},t} \leq p_{\text{Im},t} \leq P^{\max}_{\text{Im}} \cdot v_{\text{Im},t} \\
P^{\min}_{\text{Ex}} \cdot v_{\text{Ex},t} \leq p_{\text{Ex},t} \leq P^{\max}_{\text{Ex}} \cdot v_{\text{Ex},t} .
\end{aligned}
$$

b. thermal units

According to [Si, Bö] and equation (1), the shut-down (sd) and start-up (st) cost equality constraints are

$$
\begin{aligned}
C^{\text{sd}}_{j,t} \;&=\; c^{\text{sd}}_{j} \cdot z_{j,t} \text{ with a constant plant-specific value } c^{\text{sd}}_{j}, \\
C^{\text{st}}_{j,k} \;&=\; K^{\text{st}}_{j,M^{\max}} \cdot \left[v_{j,t} - \sum_{M=1}^{M^{\max}} v_{j,t-M} \right] \;\; \text{if } M \leq \left[T^{\text{cool}} + DT \right]_j .
\end{aligned} \tag{4}
$$

Equations (5) display the power constraints, wherein the segment-wise decomposition of $p_{j,t}$ is performed in appendix b. A start-up and shut-down running logic equality constraint addresses commission causality. The case $y_{j,t} = z_{j,t} = 1$ is excluded, since start-ups and shut-downs of thermal units within the same period imply both associated cost contributions $C^{\text{st}}_{j,k}$ and $C^{\text{sd}}_{j,t}$ which would contradict the goal of total ES cost

minimization. It is followed by the maximum number of accumulated daily on- and off-switching. The ramp-up and -down and power output limits indicate the flexibility of a unit [Bö],

$$\begin{aligned} P_j^{\min} \cdot v_{j,t} &\leq p_{j,t} & P_j^{\max} \cdot v_{j,t} \\ y_{j,t} - z_{j,t} &= & v_{j,t} - v_{j,t-1} \\ \sum_t y_{j,t} \leq yG_j &\text{ and } & \sum_t z_{j,t} \leq zG_j \\ p_{j,t} - p_{j,t-1} \leq r^{\text{up}} \cdot \Delta t &\text{ and } & p_{j,t-1} - p_{j,t} \leq r^{\text{do}} \cdot \Delta t. \end{aligned} \tag{5}$$

In compliance with figure (4), there are six additional constraints for minimum up- and downtimes of fossil-fueled power plants employing the commission binary variable $v_{j,t}$. They are introduced and explained in detail, see [CA], equations (21) - (26) and [Bö], pages 52 - 53. Deviating from [CA], our equations implemented in the GAMS program code include index shifts and modified initial conditions due to the underlying rolling horizon that couples hours to *days*.

c. storage facilities

The balancing equation

$$ch_{s,t} = ch_{s,t-1} + q_{s,t} \cdot \Delta t - qq_{s,t} \cdot \Delta t \text{ [e.u.]}$$

describes the storage state in t, wherein the actual charging (discharging) amount is added (subtracted) to the preceding value. For the sake of simplicity, we neglect charging and discharging efficiencies η implying that we assume zero energy losses in our model. Discharging and charging rates $disch_{s,t}$ and $charge_{s,t}$ have bounded gradients and storage filling levels are limited by $c_s^{\min} \leq ch_{s,t} \leq c_s^{\max}$.

A storage facility cannot be charged and discharged simultaneously at a certain time step t resulting in $a_{s,t} \cdot b_{s,t} = 0$ and minimized total ES costs. Since the multiplication of the two commission binary variables $\{a, b\}_{s,t} \in \{1, 0\}$ was not supported by the CPLEX solver, a logic decomposition of their product is required. It is substituted via declaring the auxiliary variable $cc_{s,t}$ in the four equations

$$\begin{aligned} cc_{s,t} \leq a_{s,t} &\text{ and } & cc_{s,t} \leq b_{s,t} \\ cc_{s,t} \geq a_{s,t} + b_{s,t} - 1 &\text{ and } & cc_{s,t} \geq 0. \end{aligned} \tag{6}$$

Although the objective function is linear, it might be necessary that a nonlinear relation is to be decoupled to avoid computational complexity during optimization. Therefore, the *standard linearization* method applies to equation (6) above that replaces the product of binary variables [T, P].

Generally, the *Glover's linearization* holds for products of binary variables x and linear functions of integer and/or continuous variables $x \cdot f(w)$ by introducing an auxiliary variable γ [T, G]. The result are four linear equations (7) visualizing up to which gradients electricity injections $q_{s,t}$ or withdrawals $qq_{s,t}$ are realized which are derived in appendix c.

d. lines

Line capacities are limited by the power inequality constraint

$$-l_{\text{sec}} \cdot LD^{\text{lim}}_{N,NP} \leq B_{N,NP} \cdot \theta_{N,NP,t} \leq l_{\text{sec}} \cdot LD^{\text{lim}}_{N,NP} \quad \forall N \neq NP \in \mathcal{N}$$

for transmitted line powers obeying a capacity security limit $l_{\text{sec}} = 70$ % for all time steps as a common thermal restriction. Therein, the voltage angle difference between two connected nodes is defined by $\theta_{N,NP,t} = da_{N,t} - da_{NP,t}$. System stability requires voltage angle boundaries $-\frac{\pi}{4} \leq da_{N,t} \leq \frac{\pi}{4}$ at each bus. By convention, N_{10} is selected as the slack bus implying $da_{N_{10},t} = 0 \, \forall t$. Analogously to water levels, a positive difference $\theta_{N,NP} > 0$ illustrates that the transmitted line power flows from a higher to a lower level. This implies positively signed line powers $LPOW_{L,t} = B_{N,NP} \cdot \theta_{N,NP,t}$ linked via the susceptance B as a proportionality constant within the DCLF approximation, as explained in [CC] and the first section.

In order to fix the initial conditions of our optimization problem, these constraints hold for $day = 1_{t=0}$.

- UC, imports or exports are impossible, $v_{\omega,0} = 0$ and $p_{\omega,0} = 0$ with $\omega = \{j, \text{ Im or Ex}\}$. The same applies to the auxiliary variables $\lambda_{i,j,0} = 0$ and $bin_{i,j,0} = 0$.
  Start-ups, shut-downs, production, emissions or costs of thermal power plants do not occur,
  $y_{j,0} = 0$, $z_{j,0} = 0$, $y^{\text{em}}_{j,0} = 0$, $C^{\text{fuel}}{}_{j,0} = 0$, $C^{\text{st}}_{j,t} = 0$.
- $\Gamma_j = 0$ and $\Lambda_j = 0$, where the parameters Γ_j and Λ_j indicate the number of inital periods of a day a unit j must be on- or offline due to its minimum up- or downtime constraint, respectively.
- No voltage angle differences are measured $\theta_{N,NP,0} = 0$ and the line powers $LPOW_{L,0}$ vanish.
- The storage facility levels are initialized to $ch_{s,0} = 0$ with $disch_{s,0} = 0$ and $charge_{s,0} = 0$.

The rolling horizon with $\phi_{day=1,\, t=24} \overset{!}{=} \phi_{day=2,\, t=0}$ and $\phi_{day=2,\, t=24} \overset{!}{=} \phi_{day=3,\, t=0}$ is employed for all variables ϕ that are fixed to zero in $day = 1_{t=0}$.

Additionally, the residual time a thermal unit j has still to run or be offline in the next day is calculated via nested loops over the indices $\{j, t\}$ for $day > 1$ by using the following conditions[7]. If a unit is started up in period t implying $v_{j,t} - v_{j,t-1} = 1$ and $t > \text{card}(t) - \text{UT}_j$ holds, then $\Gamma_j = \text{UT}_j - (\text{card}(t) - \text{ord}(t))$ is valid. In case a unit is shut down in t entailing $v_{j,t-1} - v_{j,t} = 1$ and $t > \text{card}(t) - \text{DT}_j$, then $\Lambda_j = \text{DT}_j - (\text{card}(t) - \text{ord}(t))$ applies for all time steps t. The relations for Γ_j and Λ_j are required for the first two minimum up- and downtime constraints

$$\sum_{t=1}^{\Gamma_j} [1 - v_{j,t}] = 0 \quad \text{(uptime)} \qquad \text{and} \qquad \sum_{t=1}^{\Lambda_j} v_{j,t} = 0 \quad \text{(downtime)}$$

of fossil-fueled power plants, see [CA] and [Bö], pages 52 - 53.

Case-specific conditions are imposed for scenarios like RES feed-in or demand time series variations. Particularly, line repair and thermal units' maintenance constraints allow to simulate planned outages for arbitrary time intervals.

[7] The cardinality and ordinality operators of an ordered set return its number of elements and its relative position [Ga].

3 Techno-economic scenario analysis

We present the output time series of the SCUC-OPF ES model using the DCLF approximation. The scenarios are compared qualitatively to the base case by inspecting the varied behavior of

- import, export and storage facilities
- RES feed-in: strong wind and solar eclipse
- response to line and power plant maintenance in certain time intervals.

We examine the effects on the endogenous variables

- ES total costs
- output power and commissioning state for each generator
- import and export activities at the cross-border interconnectors
- charging patterns of the storage facilities
- voltage angles and line powers.

The quantitative impacts are lucidly evaluated in subsection 3.6.

According to figure (5), wind feed-in (dark blue, dashed) is scaled-up by a factor of 1.2 (dark blue, solid) and PV feed-in underlies a temporal and regional variation. On March 20, 2015, a solar eclipse was partially visible starting at 9:30 a.m. lasting to 12:00 a.m., where the gradually distributed obscuration ranged from 80 % in the north to 65 % in the south of Germany [SR, SMA]. As a simple assumption, two cases – 70 % near N_{13} and 75 % at $N_{10,18,19}$ at 10:40 a.m. – were considered.

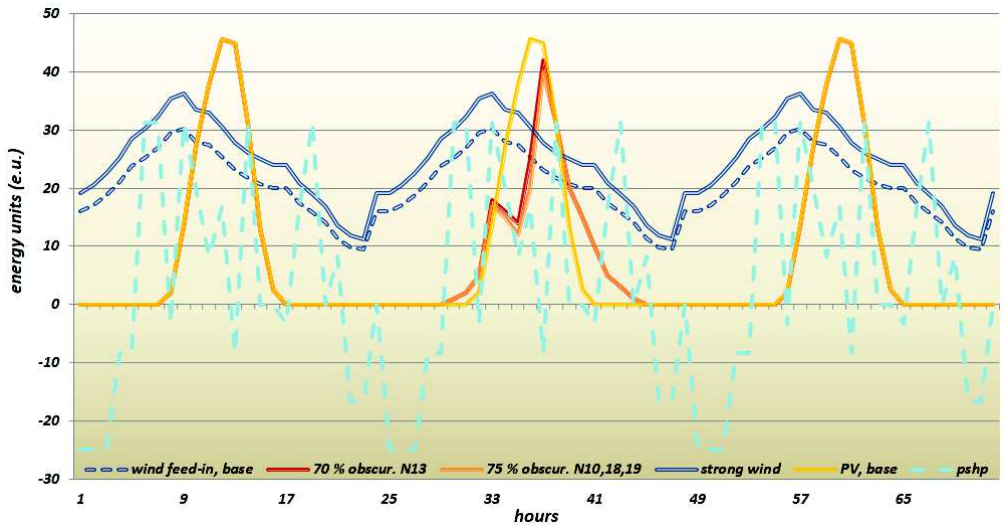

Figure 5: RES feed-in scenario input time series compared to the base case with a daily rolling horizon.

3.1 Simulation results of the reference case

In case of a symmetric output covering all three days, the first 29 optimized hours are displayed.

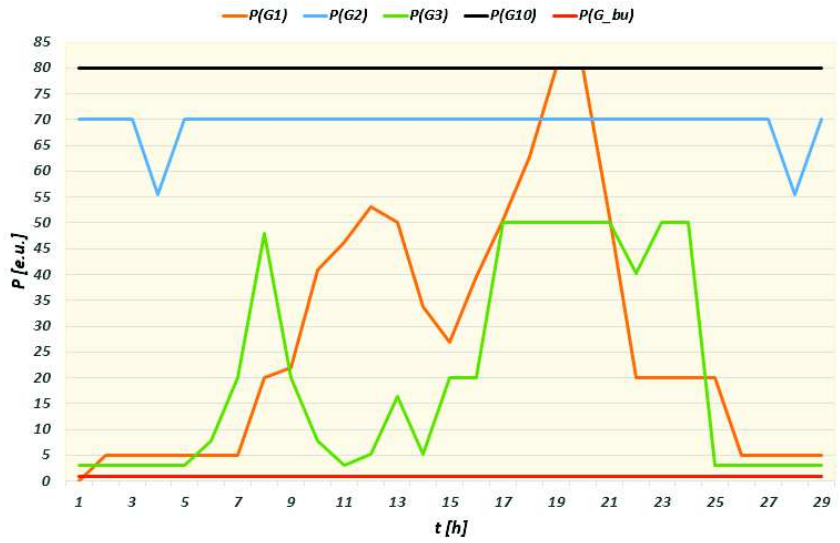

thermal unit G_j	$K^{\mathrm{st}}_{j,M^{\max}}$ [m.u.]
$\{G_1, G_2, G_3, G_4, G_5, G_6, G_7\}$	$\{14.47, 15.89, 14.31, 13.58, 13.95, 14.09, 0.04\}$
$\{G_8, G_9, G_{10}, G_{11}, G_{12}, G_{13}, G_{\mathrm{bu}}\}$	$\{10.55, 0.09, 0.09, 10.82, 10.11, 10.1, 20.83\}$

Figure 6: *top:* Exemplary fossil-fueled generators' output time series of $G_{1,2,3,10,\mathrm{bu}}$.
bottom: $K^{\mathrm{st}}_{j,M^{\max}}$ is interpreted as the plant-specific approximated start-up cost parameter. $M^{\max}$ [h] indicates a thermal unit's downtime until a start-up is possible.

Figure (6) visualizes selected profiles out of 14 thermal units operating during the entire optimization period. Obeying their particular techno-economic settings, some units react flexible indicated by spikes in the active power, whereas others supply energy constantly. According to the evolution of $p_{j,t}$ complemented by their technical characteristics, the generators are dividable into price groups.

G_{10} (black) runs permanently at its maximum power $P^{\max}_{10}$ as the "best" option of the UC. Referred to the economic quantities K^{st}_{10}, the variable, fixed, ramping and commission costs, it operates at the cheapest level. Moreover, low emissions for $\{\alpha, \beta, \gamma\}_{10}$ and a high flexibility characterized by narrow $\{UT, DT\}_{10}$ time intervals as well as a large number of allowed cumulated switching processes $\{yG, zG\}_{10}$ yield an optimal availability. Apart from an enhanced K^{st}_2 and start-up cost values, G_2 (blue) is cheap and environmentally friendly, but quite inflexible. Therefore, it shows a temporal behavior with $p_{2,t} \geq 0.78 \cdot P^{\max}_2$. $G_{1,3,6}$ with nearly identical cost and emission structures belong to the middle price class. Their supply reflects the aggregate demand profile to be balanced, where production at the limits $P^{\max,\min}_{1,3,6}$ is exploited for short time intervals. On the contrary, G_{bu} is extremely expensive, as the blatant start-up parameter $K^{\mathrm{st}}_{\mathrm{bu}}$ in figure (6) and its fixed and variable costs illustrate. On the other hand, G_{bu} is as twice as flexible as all other thermal units, due to its ramp rates and $\{yG, zG, UT, DT\}_{\mathrm{bu}}$ values. The unprofitable influence on the ES total costs combined with its advantageous technical features impels that G_{bu} runs steadily within the entire optimization horizon at its lowest output level $P^{\min}_{\mathrm{bu}}$.

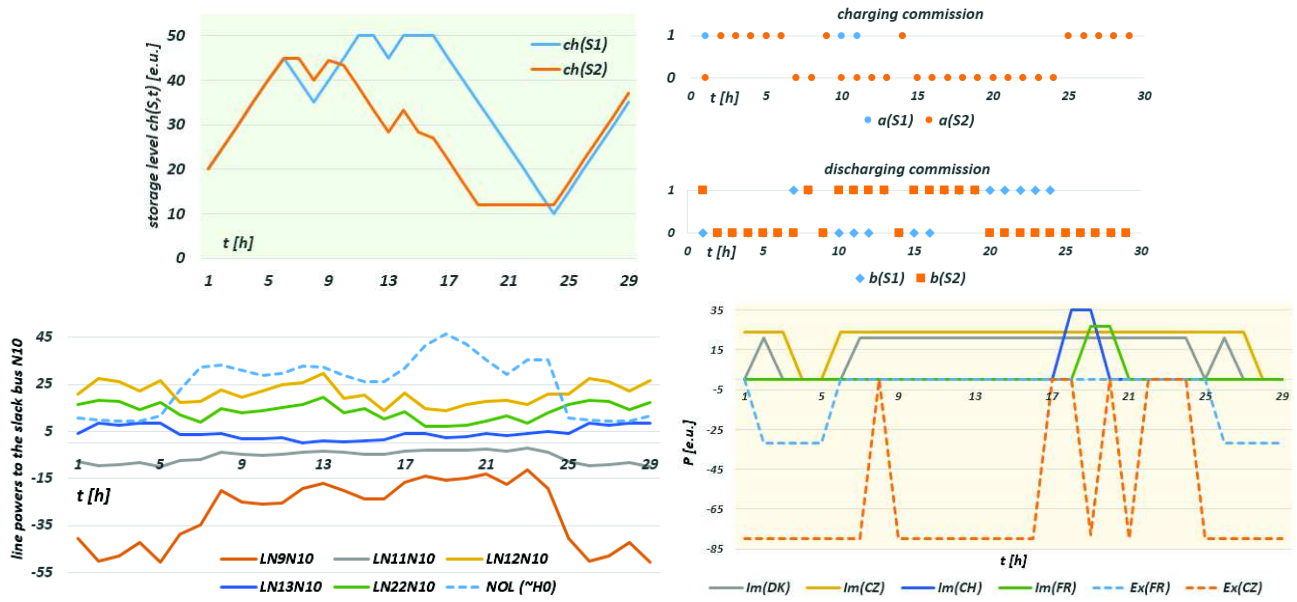

Figure 7: *top:* Time-dependent storage filling levels with capacities $c_{S_1}^{\max} = 50$ and $c_{S_2}^{\max} = 45$, $c_{S_1}^{\min} = 10$ and $c_{S_2}^{\min} = 12$ [e.u.], respectively. The binary variables $a_{s,t}$ and $b_{s,t}$ describe the commission state.
bottom left: The line powers connected to the slack bus $da_{N_{10},t} = 0$ exhibit a weakly demand profile (blue dashed) correlated trend. To account for thermal restrictions, all line capacities are limited.
bottom right: Power exchanges at the interconnectors. Export activities occur at CZ and FR due to high revenues, whereas low costs lead to imports at FR, CH, DK and CZ.

The patterns of the storage facilities S_1 (blue) and S_2 (orange) located at N_{22} and N_5 resemble because of equal (dis)charging velocities and fixed and variable costs. We inspect 5 out of 45 transmission line powers connected to the slack bus N_{10}, where several technical processes are located and a considerable amount of power feed-in takes place.

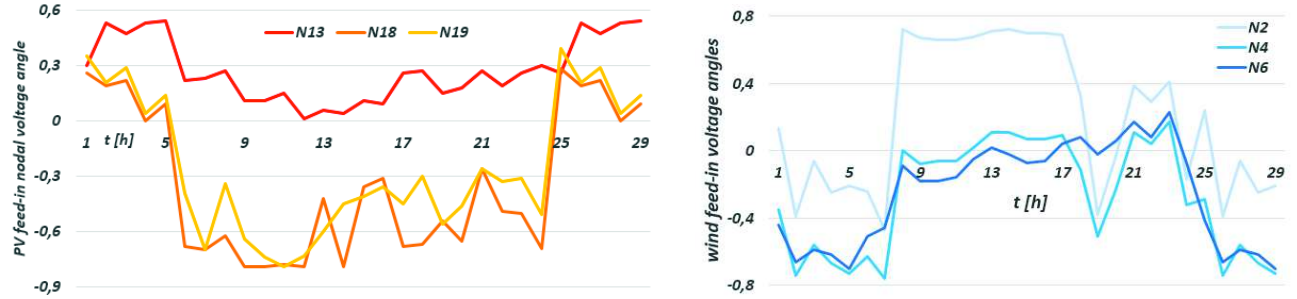

Figure 8: The nodal voltage angles for PV (left) and wind feed-in (right) are traceable to their associated underlying power profiles. In the morning ($t = 7$), the gradient is high, since the RES profiles and nodal demands rise. Discharging starts simultaneously in compliance with figures (7) and (5). Due to security constraints, all voltage angles are bounded by $\pm\frac{\pi}{4}$.

3.2 Import and export cost variation

We investigate how a variation of both variable import costs and export revenues c_{Im}^{v} and c_{Ex}^{v} by a factor of 2 and 0.5, respectively, influences the endogenous optimization variables.

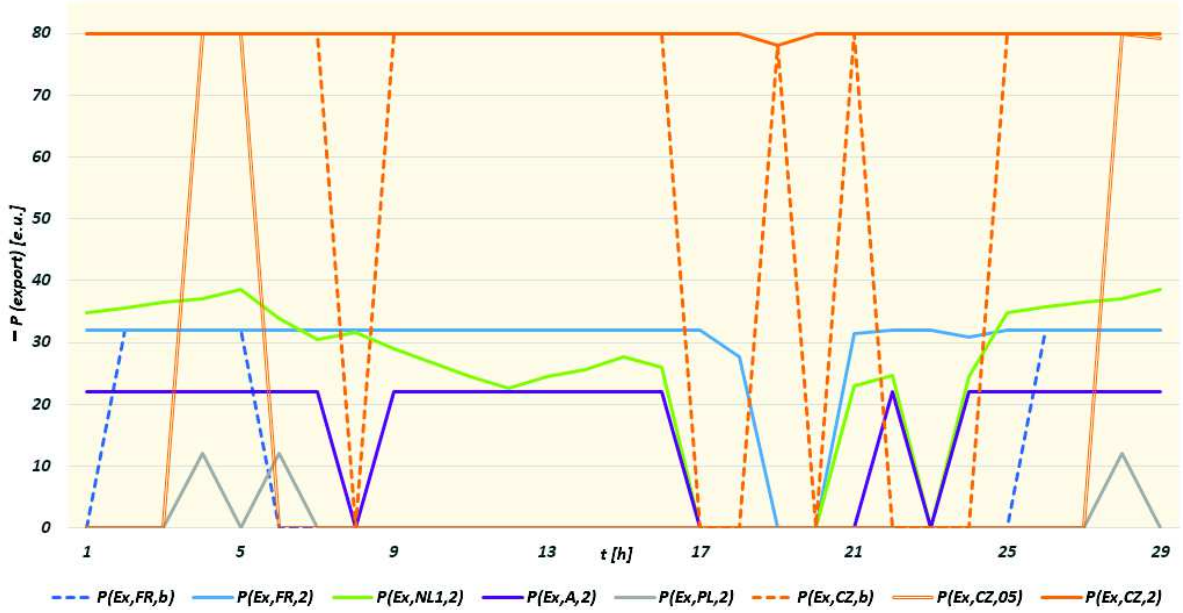

Figure 9: The export activities for halved (transparent, 05) and doubled (solid, 2) revenues c^v_{Ex} compared to the base case (dashed, b) change tremendously. Since for halved revenues c^v_{Ex}, the incentives to export shrink, purely load balancing via exports to CZ over shortened time intervals occurs. In contrast, if c^v_{Ex} double, the five countries FR, CZ, NL1, A, PL (solid, 2) export power over a longer timespan instead of FR and CZ initially participating in the benchmark scenario (dashed, b). There are tiny qualitative changes for doubled and halved import costs c^v_{Im} (not pictured).

Table (2) in subsection 3.6 reveals that for both decreased (augmented) import costs and export revenues, the ES objective increases (reduces) by an amount of 1.8 % (18 %) and the temporal aggregrated output power of the thermal units $p_{\mathbf{cum}}$ drops (raises) by 11 % (16 %), respectively.

3.3 Storage facility properties

An economic variation reflects two cases of changed storage facility variable and fixed costs by a factor of 4 and 0.25, respectively. As a technical specification, the charging and discharging gradients are increased. Whereas the simulated voltage angles, UC or transmission line powers deviate a little from the reference case, figure (10) visualizes the response of the storage facilities to different settings. Immense changes in the objective occur for an operational cost factor of 4 and 0.25, amounting to + 11 % and - 3 %, respectively.

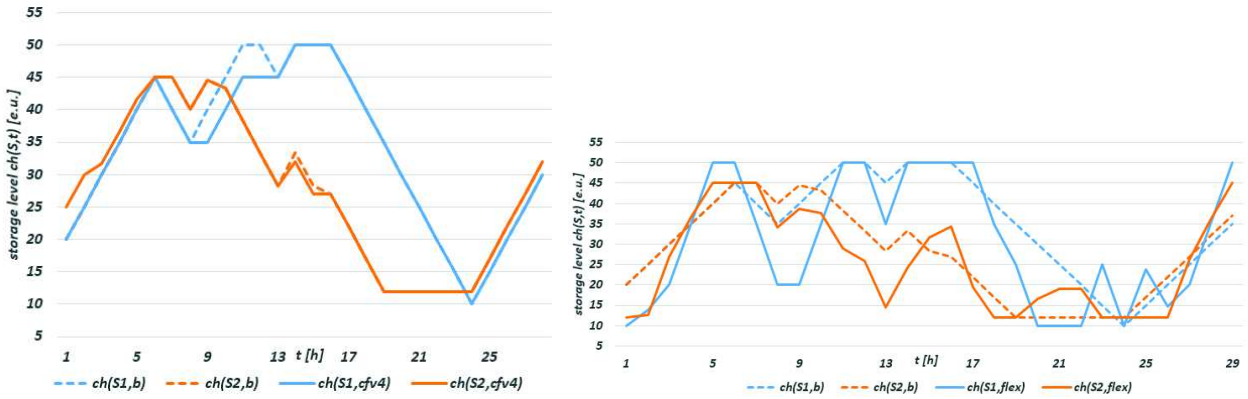

Figure 10: *left:* Charging pattern of the costly case $4 \cdot c_s^f$, $4 \cdot c_{\mathrm{ch},s}^v$ and $4 \cdot c_{\mathrm{dis},s}^v$ (solid, cfv4), where storage activities decrease for S_2 (orange) at all days and for S_1 (blue) in the mid of the first day.
right: Effect of enhanced charging and discharging gradients (1,..,5) $\rightarrow$ (1,...,15, solid, flex) $\left[\frac{\text{e.u.}}{\text{h}}\right]$. The evening spikes during $t = 5$ - 7 p.m. elicited by the demand profiles lead to maximal discharging until the lowest level $c_s^{\min}$ is reached, compare figure (1). The more adaptable (solid) the storage facility reacts to a strongly fluctuating RES supply, the steeper the level changes become.

3.4 Impact of changed RES feed-in profiles

Solar eclipse

In contrast to the prior scenarios, the solar radiation power amplitude and thus the cost function differs on the second day from the base case, see table (2) and figure (5).

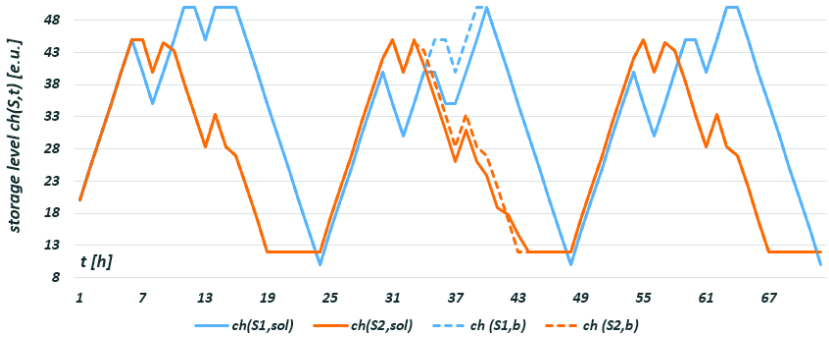

Figure 11: The peak differences reflect declined storage filling levels caused by the solar eclipse (solid, sol) occuring on the second day.

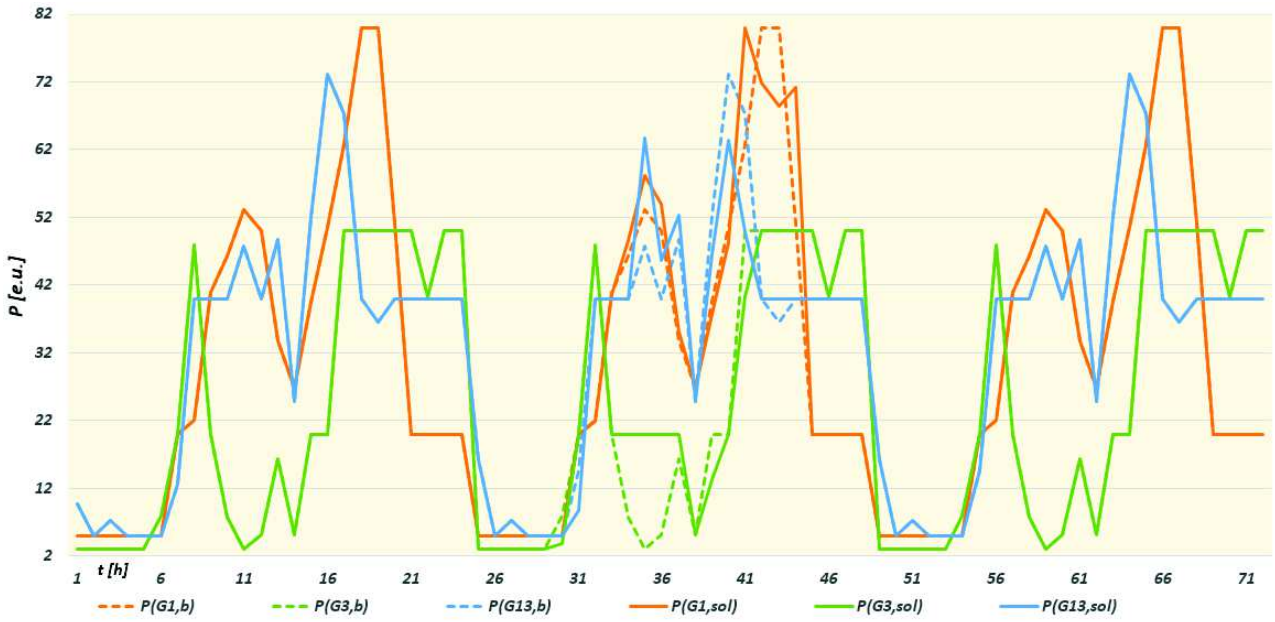

Figure 12: The power supplied by the low-priced units $G_{1,3,13}$ increases moderately to cover the load due to the deficient solar radiation on the second day (solid, sol). Most of the generators are scheduled similarly to the benchmark (dashed, b).

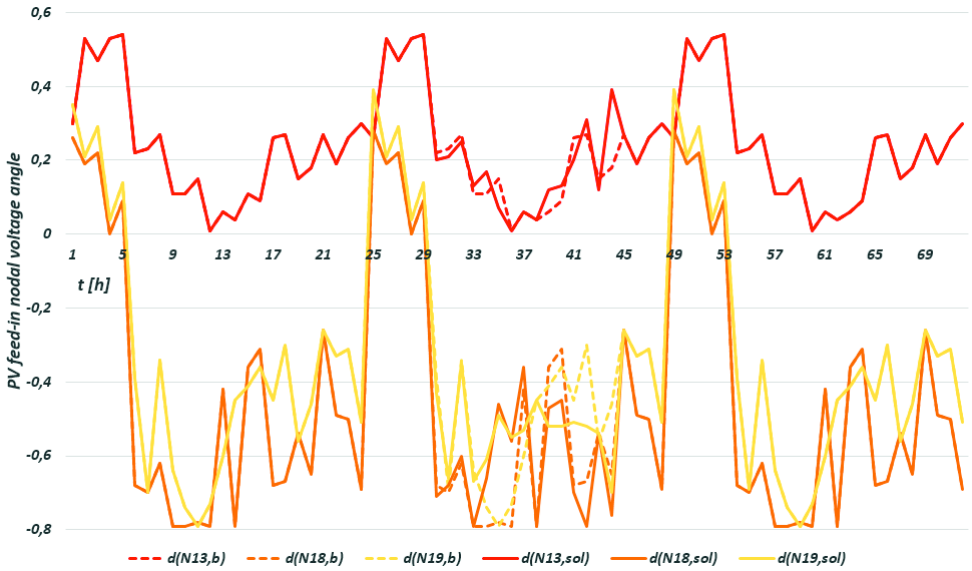

Figure 13: Voltage angles at the PV feed-in buses for the solar eclipse (solid, sol) on the second day, where at N_{13} 70 % and at $N_{18,19}$ 75 % obscuration occur, see figures (2) and (5).

Strong wind

Instead of a predictable solar feed-in, wind profiles underlie stochastic patterns such that high gradients exacerbate short-term forecasts. Figure (5) shows how the exogenous nodal wind feed-in input time series alter.

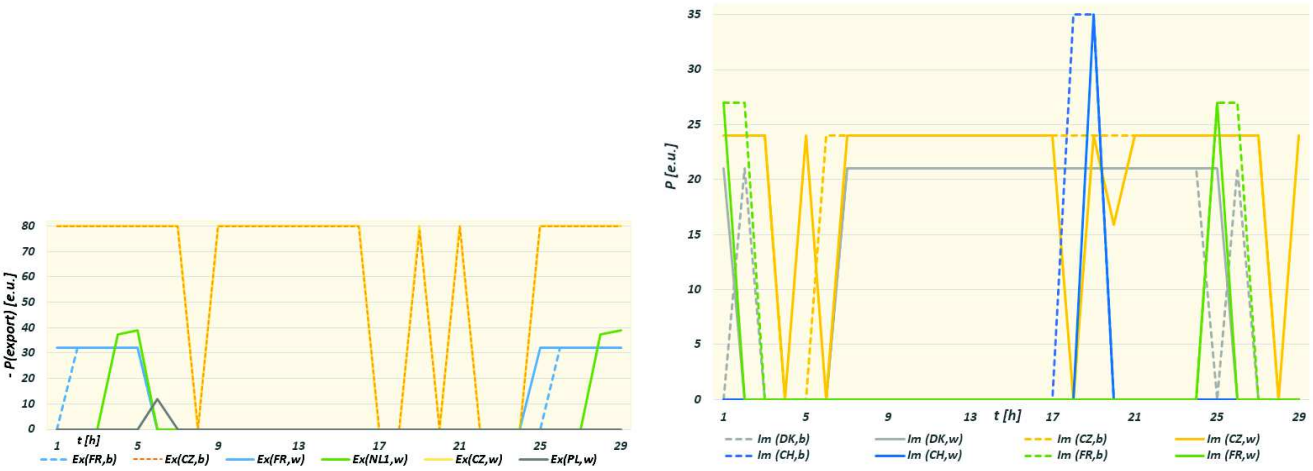

Figure 14: *left:* The up-scaled wind feed-in (solid, w) by a factor of 1.2 enhances the export activities to FR. Referred to the base case (dashed, b), additional export powers emerge at the interconnectors PL and NL1 due to an increased RES energy supply, where the interconnector CZ remains unaffected.
right: For a stronger wind feed-in (solid, w), the original import time intervals (dashed, b) narrow.

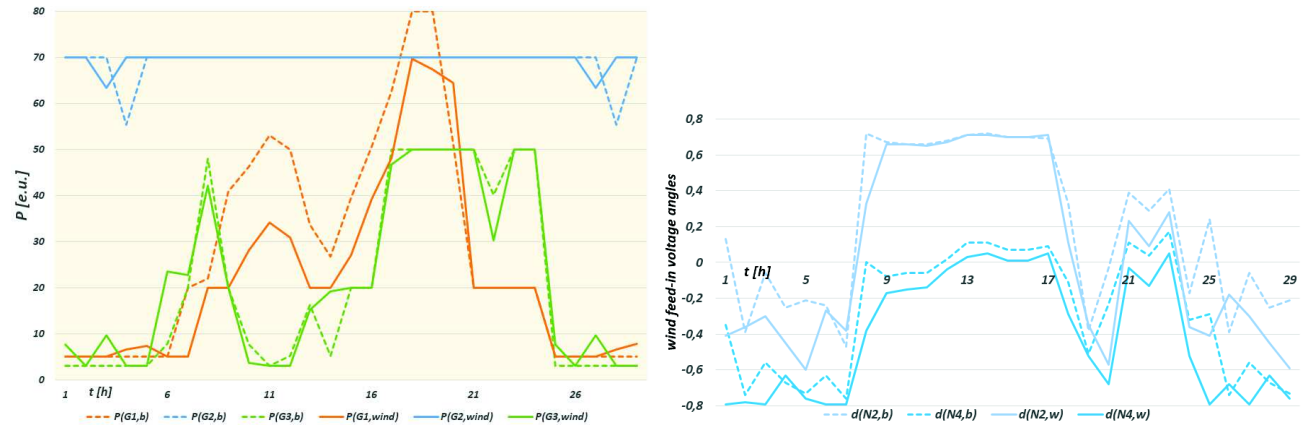

Figure 15: *left:* UC of heightened wind feed-in (solid) for the cheap unit G_2 and $G_{1,3}$ in the middle price range. The power amplitudes flatten accompanied by declined ES total costs caused by gratis wind feed-in.
right: The wind feed-in voltage angles at $N_{2,4}$ slightly smooth induced by load compensation.

3.5 Power plant maintenance and line repair

We examine the influence of switching off thermal units and lines for several hours on a certain day on the UC, ES costs as well as the voltage angles, storage levels and export capacities due to planned maintenance. In contrast to spontaneous outages involving contingency or unforeseen failures, minimum up- and downtimes or maximum counters of start-up and shut-down operational restrictions are adhered to by the units ex-ante.

Power plant repair

inputs: maintained unit	UT [h]	DT [h]	zG	yG	Δt_{repair}	*UC outputs:* $y_{j,t}$ started up	$z_{j,t}$ shut down
G_2 on $day = 1$	4	5	5	5	2 hours	$day = 1_{t=(1,10)}$	$day = 1_{t=5}$
G_{12} on $day = 2$	12	2	5	5	1 hour	$day = 1_{t=1}, day = 2_{t=11}$	$day = 2_{t=9}$

Figure 16: Start-up and shut-down commission binary variables $y_{j,t}$ and $z_{j,t}$ of the two repaired thermal units.

On the first day, G_2 (inert, cheap) is maintained during $t = 7$ and 9 a.m.. On $day = 2$, G_{12} (inflexible, middle price segment) is repaired from 9 to 10 a.m.. Overall, the fixed constraints have to be fulfilled complying with the optimal UC. Technical restrictions require that G_2 is already shut down in $t = 5$ at $day = 1$ ensuring repair during $t = 7$ - 9 a.m..

Figure (17) emphasizes that the majority of the generators retain their schedules. Several line powers and voltage angles exhibit tiny deviations during the maintenance time intervals. Export and import time series stay unaffected. The system' total costs rise by 1 % on the first day, whereas the cumulated UC powers nearly remain unchanged due to reallocation among the units.

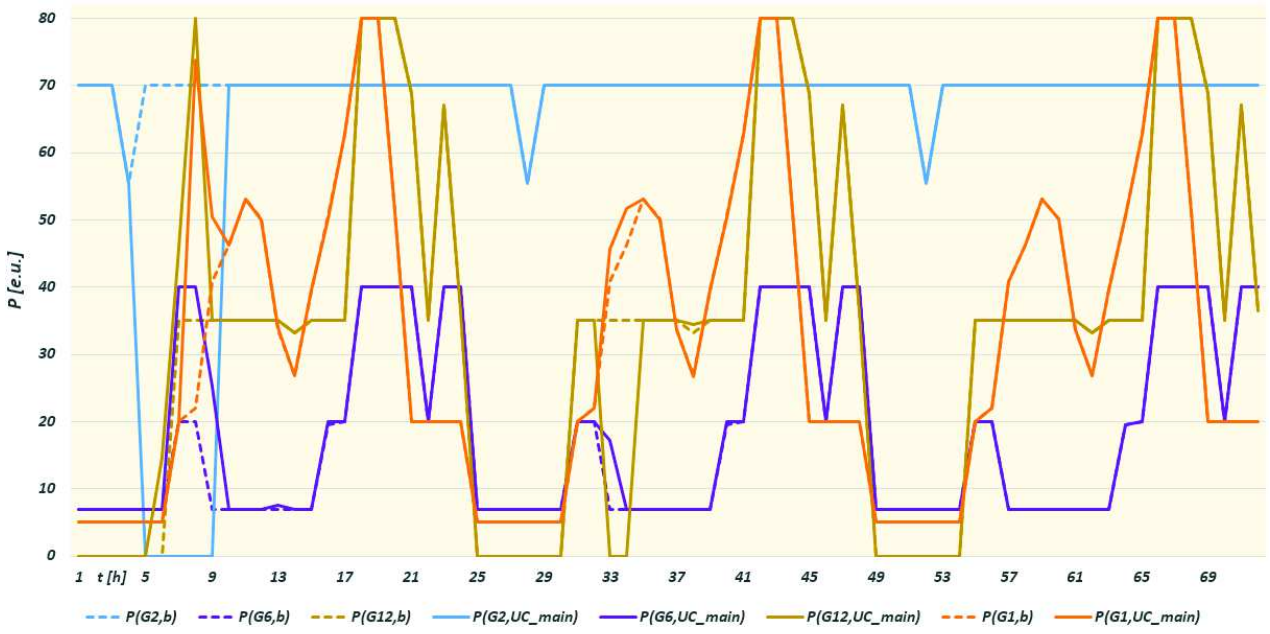

Figure 17: In comparison to the base case (dashed, b), the operating units $G_{1,6}$ endowed with similar techno-economic parameters compensate the missing power of $G_{2,12}$ during their maintenance on the first two days (solid).

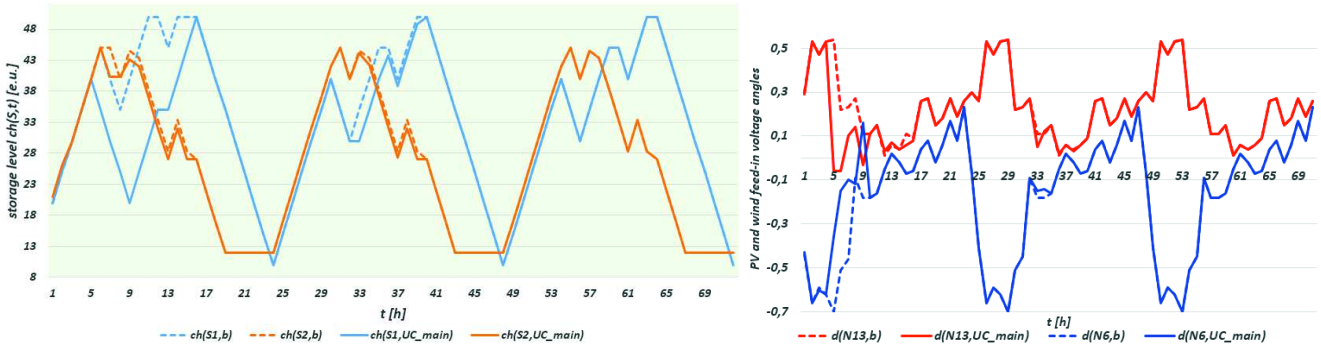

Figure 18: *left:* Less energy is stored on the first two days during the planned outages (solid) of $G_{2,12}$. *right:* The influence of power plant maintenance on the wind feed-in voltage angles (e.g. N_6) is small. For PV feed-in voltage angles (e.g. N_{13}), one observes slightly reduced values during repair (solid).

Planned line outage scenarios

scenario	lines out of operation	*day*	t [hour, a.m.]
i	$LN_{21}.N_5$	1, 2, 3	7
ii	$LN_{21}.N_5$	1, 2, 3	3 - 5
iii	$LN_{21}.N_5$	1, 2	5 - 6
	$LN_{19}.N_{21}$	2	5 - 7

Table 1: Particular lines are set out of operation for the purpose of maintenance actions. Their location is illustrated in figure (2).

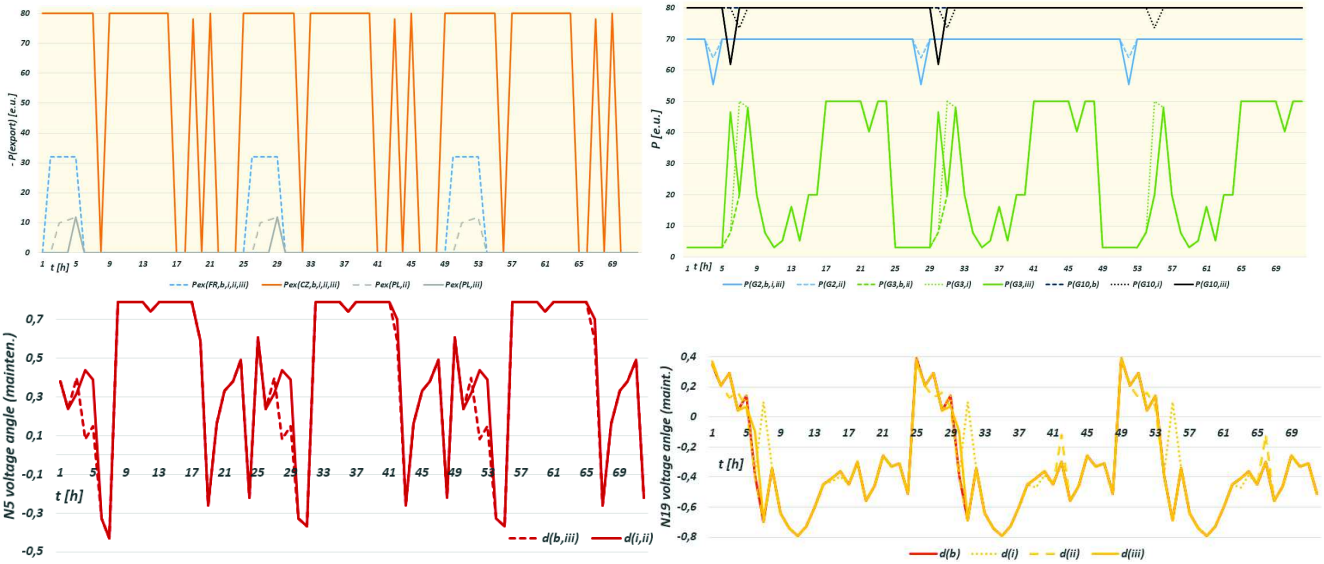

Figure 19: *top left:* For the cases ii and iii (gray), excess power is exported to PL at the affected bus N_5. *top right:* UC of the cheap $G_{2,3,10}$ during the planned line outages: except of G_3, less power is supplied. *bottom:* Whereas the scenario iii output is identical to the base case (dashed, red), the voltage angles of the buses N_5 and N_{19} located at the affected maintained lines change for i and ii, respectively.

Compared to the benchmark, small shifts in all variables are detected. Some nodal voltage angles, transmission line and import capacities and thermal units slightly alter their characteristics. The storage level patterns of S_1 equal for all cases with tiny changes for S_2 under the scenarios i and iii (not depicted).

3.6 Quantitative results

To complete this section, both the minimized total costs and thermal units' cumulated power outputs of all scenarios are depicted in table (2) which sheds light on significant systemic impacts. With respect to the choice of RES prices, parameters or normalization factors in the objective, the ES model is scaling invariant in its total cost changes under scenario deviations from the benchmark.

variation (scenario)	$goal_{day=1}$	$goal_{day=2/3}$	**trend**	**Δ**	$p_{\mathbf{cum}}$	**trend**	**Δ**
base: rounded [m.u. || e.u.]	3111	2964	reference	-	34'470	reference	-
$0.5 \cdot c^v_{\mathrm{Im}}$ and $0.5 \cdot c^v_{\mathrm{Ex}}$	3165	3018	↑	+ 54 (+ 1.8 %)	30'660	↓↓↓	- 3811 (- 11 %)
$2 \cdot c^v_{\mathrm{Im}}$ and $2 \cdot c^v_{\mathrm{Ex}}$	2576	2430	↓↓↓	- 535 (- 18 %)	40'040	↑↑↑	+ 5570 (+ 16 %)
low-cost storage $0.25 \cdot c^v_s$ and $0.25 \cdot c^f_s$	3017	2871	↓↓	- 94 (- 3 %)	34'470	-	→ 0
costly storage $4 \cdot c^v_s$ and $4 \cdot c^f_s$	3486	3339	↑↑↑	+ 375 (+ 11 %)	34'470	-	→ 0
(dis)charging rate [1...5] $\overset{\text{flex.}}{\rightarrow}$ [1...15]	3106	2959	-	→ 0	34'610	-	→ 0
solar eclipse	3111	2973 / 2964	-	→ 0	34'641	-	→ 0
"strong" 1.2 · wind feed-in	3048	2902	↓	- 63 (- 2 %)	33'651	↓↓	- 820 (- 2.5 %)
maintenance of G_2 at $day = 1_{t=7...9}$ and G_{12} at $day = 2_{t=9...10}$	3144	2965	↑ (day 1)	+ 33 (+ 1 %)	34'414	-	→ 0
planned line outages							
i $LN_{21}.N_5$ all days in $t = 7$	3113	2966	-	→ 0	34'470	-	→ 0
ii $LN_{21}.N_5$ all days in $t = 3...5$	3114	2967	-	→ 0	34'512	-	→ 0
iii $LN_{21}.N_5$ at $day = (1,2)_{t=5...6}$ and $LN_{19}.N_{21}$ at $day = 2_{t=5...7}$	3114	3114 / 2964	-	→ 0	34'441	-	→ 0

deviation	**Δ** *goal* **[m.u.]**	**trend**	**±%**	**Δ** $p_{\mathbf{cum}}$ **[e.u.]**
from ... to	**0 ... + 32 / - 32**	**→ 0**	**0 ... 1 %**	**0 ... + 345 / - 345**
within	+ (33...63) / - (33...63)	↑ / ↓	+ (1...2) % / - (1...2) %	+ (346...690) / - (346...690)
within	+ (64...94) / - (64...94)	↑↑ / ↓↓	+ (2...3) % / - (2...3) %	+ (691...1034) / - (691...1034)
beyond	+ 125 / - 125	↑↑↑ / ↓↓↓	+ 4 % / - 4 %	+ 1380 / - 1380

Table 2: *top:* Comparative evaluation of ES total costs *goal* for the scenarios c.p. all other quantities. The right columns list the results of the power values $p_{\mathrm{cum}} = \sum_{j,t,days} p_{j,t,days}$ cumulated over all units $G_{j=1,...,13,\mathrm{bu}}$ and the entire optimization period of 72 h.
bottom: Color legend of the percentage scenario scale compared to the reference case.

Varied import and export cost contributions by a factor of two, c.p. all other optimization variables, cause strong impacts on the ES costs and fossil-fueled power output, as table (2) reveals. For both decreased (augmented) import and export costs c^v_{Im} and c^v_{Ex}, the objective increases (reduces) by 1.8 %

(18 %) accompanied by a drop of 11 % (raise of 16 %) for $p_{\mathbf{cum}}$. This implies substitution effects like changed schedules of individual units and the allocation of exchange powers at the interconnectors – if export revenues double, the number of exporting countries rises.

Table (2) shows how augmented (decreased) specific costs imposed on the storage facilities effect the total costs. In case the flexibility of both storage facilities enhances by a factor of three, the gained (dis)charging gradients are exploited in order to encounter demand and RES supply.

Since a modified PV (wind) feed-in profile directly influences the load balancing equation, a higher (lower) amount of power is produced by the thermal units in total. To bridge the gap of deficient radiation due to the solar eclipse occuring on the second day, the fossil-fueled power supply by low-priced units G_j increases and the maximum storage filling levels of $S_{1,2}$ decrease at the second day, respectively. The UC in case of a strong wind feed-in reacts by lowering the power of the thermal units with a total reduction of $p_{\mathbf{cum}}$ by 2.5 %. Moreover, ES total costs decline by about 2 % caused by free feed-in accompanied by shortened import time intervals. Supplementary export activities at the interconnectors, where high revenues are realized and wind feed-in buses are located increase drastically.

The planned power plant and line outages weakly affect all endogenous variables, particularly the objective and the UC, such that many generators retain their schedules. The missing power of the maintained $G_{2,12}$ is compensated by an adapted schedule of other generators and a reduced energy storage on the first two days. Line repair actions evoke a local power surplus that is exported at the adjacent interconnector bus. Additionally, a decreased amount of power is produced in these time intervals. The three cases do not significantly influence both the objective cost function and the aggregated thermal units' power.

4 Conclusion and further research

We propose an MILP optimization model based on the SCUC-OPF formalism minimizing the ES total costs. The spatio-temporally resolved DCLF model is solved within an hourly rolling horizon approach covering three subsequent days. In order to examine different scenario constellations, it is possible to modify the underlying grid topology and to include or remove technology combinations and multiple flexibility options located at certain buses for a desired duration. More precisely, nodal import and export activities, storage facilities, thermal power plants and PSHP, demand profiles, exogenous wind and PV feed-in as well as an extended rolling optimization horizon including a free choice of time slices are integrable arbitrarily.

The central research questions address the study of the system's response by inspecting endogenous variable time series such as voltage angles, line powers, the UC and the commissioning state for each power generator or storage unit represented by binary variables, the temporal behavior of the import and export time series as well as the charging patterns of storage facilities. Additionally, systemic effects of line repair and power plant maintenance across several hours on special days are examined. We suggest a high and variable power system resolution from an interlinked techno-economic and ecological perspective. The provided tool integrates technical (stability and flexibility), ecological (output power-dependent emissions of thermal units and predominant RES feed-in) and economic (technology-specific fixed and variable costs or nodal price time series) aspects. Compared to other ES modeling approaches in literature [E, SW], the thermal units were parametrized in detail exploiting piecewise approximations and linearization procedures such that the objective function depends solely linearly on the optimization variables. The model is

endowed by security-limited power line properties characterized by length-dependent susceptances, thermal limits as well as endogenized storage facilities described by capacity limits, charging and discharging rates. The linearization applied to the start-up costs and the directly linked production power and emissions of fossil-fueled power plants is a value-added, since with an enhanced number of breakpoints, the model can be finetuned. Therefore, the high degrees of freedom allow scalability of the network topology and techno-economic model specifications. Besides, the system's total costs are extendable by process terms that fit into the mixed-integer optimization framework.

The sensitivity and cost differentials of the objective function against altered optimization variables (c.p.) can be derived from our study. We conclude that monetary incentives set on imports and exports strongly influence the ES total costs accompanied by substitution effects of specific units within the scheduled UC and a reallocation of exchange activities at the interconnector buses. It can be derived that apart from high development expenses, an enhanced flexibility of storage facilities is advantageous in order to balance a fluctuating RES feed-in and load gradients. Moreover, we find that changed wind or PV feed-in power profiles influence the UC of thermal units and the nodal angles offset by deviating temporal storage and import or export patterns. Maintenance actions of thermal units and lines lead to local effects revealed by the compensatory behavior of the endogenous variables within the simulated repair time intervals.

Future research is twofold comprising both technical model extensions (I) and adaptions closer to reality (II) that imply the following issues.

(I) An inspiring task concerns the study of unplanned successive line failures or fossil-fueled power plant outages in the framework of contingency analysis to examine supply security by applying stochastic optimization modeling methods [O, HG]. Furthermore, it is beneficial to endogenize PSHP generation, where pumping and turbining processes are represented by storage equations, as performed in [E]. This method is extended in [SW], where an electricity market model of Switzerland combining a hydropower system (run-of-river, PSHP and storage) with a DCLF network representation reveals the location of bottlenecks by means of evaluating nodal prices. In addition, length-dependent line losses associated to specific costs are worth to be estimated. Since losses depend on the power transmitted over a line, they can be summed up entering as cost terms into the objective. Moreover, inspecting the effects of electric vehicles on the grid stability of a power system is a desirable topic [K].

(II) Exploiting the technical modeling features of this work, an [MW, €]-calibration to existing power systems on a national level incorporating rescaled specifications of storage facilities, power plants and lines, as well as real actual numerical values is appropriate. Besides, taking into account high-voltage DC grid structures, underground cables or scenarios based on the German Grid Development Plan, improves the understanding of transmission grid extensions or bottlenecks in the field of congestion management. However, for urban ES, the ACLF method is an adequate choice to assess voltages, currents and reactive powers at lower voltage levels. Sector coupling models embedding power-to-gas conversion gain higher relevance in the next years for optimal infrastructure planning. Finally, investigating electricity market designs under debate such as locational marginal or zonal pricing with regard to flexibility options and grid reliability, paves the way to assess systemic welfare effects on a national level, as suggested in [ST, E, Öz, DF, ÖH].

Appendix

a Additive parallel susceptances

Consider an electric circuit of two parallel wires of constant voltage $U_k = U$ and differing currents I_k. By Kirchhoff's law, currents are compensated at a node k due to charge conservation, $\sum_k I_k = 0 \rightarrow I_1 + I_2 = I_{\text{tot}}$. This relation can be expressed by the product of admittance and voltage, $\sum_k Y_k U_k = 0$. In our case, it follows $Y_{\text{tot}} U = Y_1 U + Y_2 U \rightarrow Y_{\text{tot}} = Y_1 + Y_2$.

For an arbitrary number of parallel complex-valued admittances, $\underline{Y}_k \in \mathbb{C}$ are decomposed into conductance G_k and susceptance B_k such that $\underline{Y} = \sum_k \underline{Y}_k = \sum_k G_k + j \sum_k B_k$ holds with the imaginary unit $j = \sqrt{-1}$. Hence, admittances (susceptances) sum up in parallel circuits.

b Piecewise linearization of thermal units' production and emission functions

We apply a linearization concept of the OPF generation fuel cost function

$$C_j^{\text{prod}} = f_j(p_j) = (\delta_j + \epsilon_j p_{j,t} + \kappa p_{j,t}^2)$$

using a piecewise set of blocks by exploiting the λ-formulation, where any point between two breakpoints is the weighted sum of these neighboring values [P]. For the sake of simplicity, time and power plant indices j, t are suppressed. As stated in [P], the following assumptions hold for the positive weighting factors λ_i. $\sum_i \lambda_i = 1 (i)$ such that the linear approximation of the function values $\widetilde{f}(p) = \sum_i \lambda_i f(p_i) (ii)$ is fulfilled with $\sum_i \lambda_i p_i = p \, (iii)$. An additional requirement using binary variables is that at most two adjacent $\lambda_i > 0 \, (iv)$ which is redundant in our case. The mathematical background is that the function to minimize $f(p)$ is separable and convex characterized by successive non-decreasing, piecewise linear approximated slopes. If the considered function is non-convex, the adjacency requirement (iv) is mandatory [P]. The constraints above guarantee that for all separable functions defined as the sum of functions of scalar variables, $(p, \widetilde{f}(p))$ lie on the approximated line segments.

According to figure (3, left), we implemented the case $i = \{1, 2, 3\}$ at $p_j = \{P^{\min}, P^a, P^{\max}\}_j$ comprising two segments. Note that the number of breakpoint power values is freely selectable in the model. Thus, the parameters are set

$$\begin{aligned} pval_{i=1,2,3,j,t} &= P_j^{\min,a,\max} \\ yval_{i,j,t} &= \underbrace{A}_{\delta_j} + \underbrace{B}_{\epsilon_j} \cdot pval_{i,j,t} + \underbrace{10^{-4} B}_{\kappa_j} \cdot pval_{i,j,t}^2 \quad \forall t > 1. \end{aligned}$$

The variables $C_{j,t}^{\text{fuel}}$, $\lambda_{i,j,t}$, $p_{j,t}$ and $bin_{i,j,t}$ are introduced for the modeling equations (i') – (iv'') and the bounded linearly approximated output power

$$p_{j,t} = \sum_i \lambda_{i,j,t} \cdot pval_{i,j,t} \quad (iii').$$

We define a set $\text{notlast}_{i,j,t}$ satisfying the condition $\text{ord}(i) < \text{card}(i)$ implying $\text{card}(i) = 3$ and $\text{ord}(i) = \{1, 2\}$ in our case. The equations related to piecewise linear approximated emissions and production costs are denoted by

$$
\begin{aligned}
\sum_{i=1,2,3} \lambda_{i,j,t} &= 1 \quad (i') \\
C^{\text{prod}}_{j,t} \approx C^{\text{fuel}}_{j,t} &= \sum_{i} \lambda_{i,j,t} \cdot yval_{i,j,t} \quad (ii') \\
y^{\text{em}}_{j,t} &= \sum_{i} \lambda_{i,j,t} \cdot y^{\text{em}}val_{i,j,t} \quad (ii'') \\
\lambda_{i,j,t} &\leq bin_{i-1,j,t} + bin_{i,j,t}\$\text{notlast}_{i,j,t} \quad (iv') \\
\text{with } \lambda_{2,j,t} &\leq bin_{1,j,t} + bin_{2,j,t} \quad \text{and} \quad \lambda_{3,j,t} \leq bin_{2,j,t} \\
\sum_{i\$\text{notlast}_{i,j,t}} bin_{i,j,t} = bin_{1,j,t} + bin_{2,j,t} &= 1 \quad (iv'').
\end{aligned}
$$

Using this formulation, they are implemented into the GAMS program code.

The parametrization of the scaled emission function

$$E_j(p_{j,t}) = \left\{ \alpha_j + \beta_j \cdot p_{j,t} + \gamma_j \cdot p^2_{j,t} + \zeta_j e^{\psi_j p_{j,t}} \right\}$$

is deduced from [SM], section 5.3.1.5 with emission coefficient values taken from table A.3, page 341. In the model, we chose

$$y^{\text{em}}val_{i,j,t} = \alpha_j + \beta_j \cdot pval_{i,j,t} + \gamma_j \cdot pval^2_{i,j,t}$$

as the parameter for its quadratic approximation leading to equation (ii'').

c Glover's linearization of charging and discharging rate equations

The product $x \cdot f(w)$ introducing the auxiliary variable γ [T] is expressed by

$$f(w)^{\min} \leq \gamma \leq f(w)^{\max} \quad \text{(I)} \quad \text{and} \quad f(w) - f(w)^{\max}(1-x) \leq \gamma \leq f(w) - f(w)^{\min}(1-x) \quad \text{(II)}.$$

In our case, there are products of binary $x \rightarrow \{a_{s,t}, b_{s,t}\}$ and continuous $f(w) \rightarrow \{charge_{s,t}, disch_{s,t}\}$ variables, $a_{s,t} \cdot charge_{s,t}$ and $b_{s,t} \cdot disch_{s,t}$ with

$$f(w)^{\min} \rightarrow \{Cl_s \cdot a_{s,t}, DISl_s \cdot b_{s,t}\} \quad \text{and} \quad f(w)^{\max} \rightarrow \{CH_s \cdot a_{s,t}, DIS_s \cdot b_{s,t}\}.$$

Therein, the lower bounds of charging and discharging amounts $q_{s,t}$ and $qq_{s,t}$ of a storage facility s in a time period t are denoted by Cl_s and $DISl_s$. The upper intake and withdrawal limits are given by CH_s and DIS_s $\left[\frac{\text{e.u.}}{\text{h}}\right]$. The set of charging and discharging equations are linearized and the positive auxiliary variables $\gamma \rightarrow \{q_{s,t}, qq_{s,t}\}$ are inserted into

$$
\begin{aligned}
Cl_s \cdot a_{s,t} &\leq q_{s,t} \quad \text{and} \quad q_{s,t} \leq CH_s \cdot a_{s,t} \quad \text{bounded charging rates} \\
DISl_s \cdot b_{s,t} &\leq qq_{s,t} \quad \text{and} \quad qq_{s,t} \leq DIS_s \cdot b_{s,t} \quad \text{bounded discharging rates} \quad \text{(I)},
\end{aligned}
$$

yielding the four decoupled expressions

$$
\begin{aligned}
charge_{s,t} - Cl_s \cdot [1 - a_{s,t}] &\geq q_{s,t} \quad \text{and} \quad charge_{s,t} - CH_s \cdot [1 - a_{s,t}] \leq q_{s,t} \\
disch_{s,t} - DISl_s \cdot [1 - b_{s,t}] &\geq qq_{s,t} \quad \text{and} \quad disch_{s,t} - DIS_s \cdot [1 - b_{s,t}] \leq qq_{s,t} \quad \text{(II)} \quad \forall t > 1. \qquad (7)
\end{aligned}
$$

d Computational performance

The exogenous time-dependent inputs in figures (1) and (5) are collected in EXCEL datasheets and transformed into tables imported in the program code of the ES model. The datasheets are converted into .inc files that can be processed by GAMS. After solving the model, the .csv-files including clustered output time series are readable in EXCEL again.

The time-dependent levels $.l$ of these endogenous quantities and parameters are displayed after solving,

- $goal$, $B_{N,NP}$, $\theta_{N,NP,t}$, $da_{N,t}$, $ch_{s,t}$, $a_{s,t}$, $b_{s,t}$, $\lambda_{i,j,t}$, $bin_{i,j,t}$, $yval_{i,j,t}$, $y^{\mathrm{em}}_{j,t}$, $y^{\mathrm{em}}val_{i,j,t}$, $M^{\max}_{j}$, $K^{\mathrm{st}}_{j,M^{\max}}$,
- $v_{j,t}$, $v_{\mathrm{Im},t}$, $v_{\mathrm{Ex},t}$, $p_{j,t}$, $p_{\mathrm{Im},t}$, $p_{\mathrm{Ex},t}$, $y_{j,t}$, $z_{j,t}$, zG_j, yG_j, $C^{\mathrm{fuel}}_{j,t}$, $C^{\mathrm{st}}_{j,t}$, $C^{\mathrm{sd}}_{j,t}$, $LPOW_{L,t}$.

The CPLEX solver for MIP programming of the GAMS version 24.7.1 was used with the settings

- $optcr = 10^{-4}$ given by Δ(best possible - any final solution)
- maximal iterations until abortion $iterlim = 10^8$ and $reslim = 10^{10}$.

e Nomenclature

acronym	***term***
SC(UC)	security-constrained (unit commitment)
ACLF, DCLF	alternating current load flow, direct current load flow
OPF	optimal power flow
MI[N](L)P	mixed-integer [non-](linear) programming
GAMS CPLEX	General Algebraic Modeling System (software) GAMS solver, optimization software package
RES	renewable energy sources
PSHP	pumped-storage hydro power
PV	photovoltaics
DK, CH, CZ, FR, A, PL, NL	Denmark, Switzerland, Czech Republic, France, Austria, Poland, The Netherlands
ES	energy system
m.u.	monetary units [EUR, $]
e.u.	energy units [kW, MW] for active powers P
EEG	Renewable Energy Sources Act (German: Gesetz für den Ausbau erneuerbarer Energien, Erneuerbare-Energien-Gesetz)
c.p.	ceteris paribus
bu	back up
symbol	***notation in electrical engineering***
$j = \sqrt{-1}$	imaginary unit for complex-valued quantities
N, NP, k, m and km	adjacent buses (nodes) and transmission power line
$S^{\mathrm{AC}}_k = P^{\mathrm{AC}}_k + jQ^{\mathrm{AC}}_k$	complex-valued apparent power consisting of real active and imaginary reactive power contributions
U_k and I_k	voltage and electric current
$y_{km} = (g_{km} + jb_{km})$	complex-valued admittance consisting of real conductance and imaginary susceptance
$z_{km} = (r_{km} + jx_{km})$	complex-valued impedance consisting of real (ohmic) resistance and imaginary reactance
$\theta_{km} = \theta_k - \theta_m = da_k - da_m$	voltage angle difference between two nodes

References

[B] R. Bacher, *Power System Models, Objectives and Constraints in Optimal Power Flow Calculations* (in *Optimization in Planning and Operation of Electric Power Systems*), **217-64**, Physica-Verlag (Springer), (1993).

[Bi] D. Bienstock, *Progress on solving power flow problems*, Mathematical Optimization Society Newsletter, OPTIMA, Issue **93**, (2013).

[Bö] D. Böttger, *Energiewirtschaftliche Auswirkungen der Power-to-Heat-Technologie in der Fernwärmeversorgung bei Vermarktung am Day-ahead Spotmarkt und am Regelleistungsmarkt*, Dissertation Universität Leipzig, (2017).

[CA] M. Carrion, J. M. Arroyo, *A Computationally Efficient Mixed-Integer Linear Formulation for the Thermal Unit Commitment Problem*, IEEE Transactions on Power Systems **21(3): 1371-8**, (2006).

[CC] E. Castillo et al., *Building and Solving Mathematical Programming Models in Engineering and Science*, Wiley, (2002).

[D] T. Drees, *Dispatch optimization of thermal power plants considering non-linear constraints*, Presentation RWTH Aachen, (2015).

[DF] F. Ding, J. D. Fuller, *Nodal, Uniform, or Zonal Pricing: Distribution of Economic Surplus*, IEEE Transactions on Power Systems, **Vol. 20 (2)**, **875-82**, (2005).

[E] J. Egerer, *Open Source Electricity Model for Germany (ELMOD-DE)*, DIW Data Documentation 83, Berlin, (2016).

[EA] Electricity Authority, New Zealand, *Grid reliability standards*, `https://www.ea.govt.nz/operations/transmission/grid-reliability-standards/`, accessed (06/2018).

[EC] Commission of the European Communities, *Green Paper – A European Strategy for Sustainable, Competitive and Secure Energy {SEC(2006) 317}*, Brussels, 2006, `http://europa.eu/documents/comm/green_papers/pdf/com2006_105_en.pdf`, accessed (07/2018).

[Ei] J. Eickmann et al., *Optimizing Storages for Transmission System Operation,* Energy Procedia, 8th International Renewable Energy Storage Conference and Exhibition, IRES 2013, **Vol. 46: 13-21**, (2014).

[F] Y. Fu et al., *Security-Constrained Unit Commitment With AC Constraints,* IEEE Transactions on Power Systems **20(3): 1538-50**, (2005).

[FR] S. Frank, S. Rebennack, *A Primer on Optimal Power Flow: Theory, Formulation and Practical Examples*, Working Paper No. 2012-14, Colorado School of Mines, (2012).

[G] F. Glover, *Improved Linear Integer Programming Formulations Of Nonlinear Integer Problems*, Management Science **22(4): 455-60**, (1975).

[Ga] GAMS Documentation Center 25.1, `https://www.gams.com/latest/docs/UG_OrderedSets.html#UG_OrderedSets_OrdAndCard`, accessed (06/2018).

[Gr] M. Groschke et al., *Neue Anforderungen an optimierende Energiesystemmodelle für die Kraftwerkseinsatz- und Zubauplanung bei begrenzten Netzkapazitäten*, Zeitschrift für Energiewirtschaft, **33(1): 14-22**, (2009).

[H] E. Handschin et al., *Optimaler Kraftwerkseinsatz in Netzengpasssituationen* (in *Innovative Modellierung und Optimierung von Energiesystemen*, Ed.: R. Schultz, H. J. Wagner), LIT-Verlag, (2009).

[HG] V. Hinojosa, F. Gonzalez-Longatt, *Stochastic security-constrained generation expansion planning methodology based on a generalized line outage distribution factors*, IEEE Manchester PowerTech Conference, (2017).

[K] G. Kaestle et al. *Smart Standards for Smart Grid Devices*, Conference Paper, (2011).

[Kr] T. Kristiansen, *Utilizing MATPOWER in Optimal Power Flow,* Modeling, Identification and Control, **Vol. 24(1): 49-59**, (2003).

[N] C. Nolden et al., *Network constraints in techno-economic energy system models: towards more accurate modeling of power flows in long-term energy system models,* Energy Systems, Springer-Verlag Berlin Heidelberg, **Vol. 4(3): 1290-1300**, (2013).

[O] M. Ovaere, *Electricity Transmission Reliability Management*, IAEE Energy Forum, (2016).

[ÖH] K. Östman, M. R. Hesamzadeh, *Transmission Pricing in Interconnected Systems – A Case Study of the Nordic Countries*, ENERGYCON, Croatia, (2014).

[Öz] Ö. Özdemir et al., *A Nodal Pricing Analysis of the Future German Electricity Market*, IEEE EEM Conference Paper, (2009).

[P] AIMMS B.V., *AIMMS Modeling Guide – Integer Programming Tricks (Chapter 7)*, `https://download.aimms.com/aimms/download/manuals/AIMMS3OM_IntegerProgrammingTricks.pdf`, accessed (06/2018).

[R] RGCE SG Network Models and Forecast Tools, *Indicative values for Net Transfer Capacities (NTC) in Continental Europe*, `http://www.entsoe.eu/fileadmin/user_upload/_library/ntc/archive/NTC-Values-Winter-2010-2011.pdf`, accessed (06/2018).

[Sch] M. Schönfelder et al., *New Developments in Modeling Network Constraints in Techno-economic Energy System Expansion Planning Models*, Zeitschrift für Energiewirtschaft **36: 27-35,** (2012).

[SH] T. F. Slaper, T. J. Hall, *The Triple Bottom Line: What Is It and How Does It Work?,* Indiana Business Review **86 (1)**, 2011, `http://www.ibrc.indiana.edu/ibr/2011/spring/article2.html`, accessed (07/2018).

[Si] M. Silbernagl et al., *Improving Accuracy and Efficiency of Start-up Cost Formulations in MIP Unit Commitment by Modeling Power Plant Temperatures*, IEEE Transactions on Power Systems **31(4): 2578-86**, (2016).

[SM] S. A.-H . Soliman, A.-A. H. Mantawy, *Modern Optimization Techniques with Applications in Electric Power Systems (Chapter 5)*, Springer, (2012).

[SMA] SMA Solar Technology AG, *Das leistet Photovoltaik in Deutschland, Relative Leistung vom 20.03.2015, Tagesgang der PV-Leistung in Deutschland*, `https://www.sma.de/unternehmen/pv-leistung-in-deutschland.html`, accessed (06/2018).

[SR] Landeshauptstadt Stuttgart, Amt für Umweltschutz, Abt. Stadtklimatologie, `https://www.stadtklima-stuttgart.de/index.php?klima_kalender_ereignisse_sofi_2015`, accessed (05/2018).

[ST] H. Stigler, C. Todem, *Optimization of the Austrian Electricity Sector (Control Zone of VERBUND APG) under the Constraints of Network Capacities by Nodal Pricing*, CEJOR **13(2): 105-25**, (2005).

[Ste] B. Stern, *Kraftwerkseinsatz und Stromhandel unter Berücksichtigung von Planungsunsicherheiten*, Dissertation RWTH Aachen, (2001).

[Sto] B. Stott et al., *DC Power Flow Revisited,* IEEE Transactions on Power Systems, **Vol. 24(3): 1290-1300**, (2009).

[SW] I. Schlecht, H. Weigt, *Swissmod – A Model of the Swiss Electricity Market*, WWZ Discussion Paper, University of Basel, (2014).

[T] M. Theofilidi, *Development of a mixed-integer optimization model for unit commitment and its application to the German electricity market*, Master Thesis TU Berlin, (2008).

[Ta] E. Talebizadeh et al., *Evaluation of plug-in electric vehicles impact on cost-based unit commitment*, Journal of Power Sources **248 (545-52)**, (2014).

[W] B. Wright, *A Review of Unit Commitment,* ELENE 4511, (2013).

Universität Leipzig
Wirtschaftswissenschaftliche Fakultät

Nr. 1	Wolfgang Bernhardt	Stock Options wegen oder gegen Shareholder Value? Vergütungsmodelle für Vorstände und Führungskräfte 04/1998
Nr. 2	Thomas Lenk / Volkmar Teichmann	Bei der Reform der Finanzverfassung die neuen Bundesländer nicht vergessen! 10/1998
Nr. 3	Wolfgang Bernhardt	Gedanken über Führen – Dienen – Verantworten 11/1998
Nr. 4	Kristin Wellner	Möglichkeiten und Grenzen kooperativer Standortgestaltung zur Revitalisierung von Innenstädten 12/1998
Nr. 5	Gerhardt Wolff	Brauchen wir eine weitere Internationalisierung der Betriebswirtschaftslehre? 01/1999
Nr. 6	Thomas Lenk / Friedrich Schneider	Zurück zu mehr Föderalismus: Ein Vorschlag zur Neugestaltung des Finanzausgleichs in der Bundesrepublik Deutschland unter besonderer Berücksichtigung der neuen Bundesländer 12/1998
Nr: 7	Thomas Lenk	Kooperativer Förderalismus – Wettbewerbsorientierter Förderalismus 03/1999
Nr. 8	Thomas Lenk / Andreas Mathes	EU – Osterweiterung – Finanzierbar? 03/1999
Nr. 9	Thomas Lenk / Volkmar Teichmann	Die fisikalischen Wirkungen verschiedener Forderungen zur Neugestaltung des Länderfinanz-ausgleichs in der Bundesrepublik Deutschland: Eine empirische Analyse unter Einbeziehung der Normenkontrollanträge der Länder Baden-Würtemberg, Bayern und Hessen sowie der Stellungnahmen verschiedener Bundesländer 09/1999
Nr. 10	Kai-Uwe Graw	Gedanken zur Entwicklung der Strukturen im Bereich der Wasserversorgung unter besonderer Berücksichtigung kleiner und mittlerer Unternehmen 10/1999
Nr. 11	Adolf Wagner	Materialien zur Konjunkturforschung 12/1999
Nr. 12	Anja Birke	Die Übertragung westdeutscher Institutionen auf die ostdeutsche Wirklichkeit – ein erfolg-versprechendes Zusammenspiel oder Aufdeckung systematischer Mängel? Ein empirischer Bericht für den kommunalen Finanzausgleich am Beispiel Sachsen 02/2000
Nr. 13	Rolf H. Hasse	Internationaler Kapitalverkehr in den letzten 40 Jahren – Wohlstandsmotor oder Krisenursache? 03/2000
Nr. 14	Wolfgang Bernhardt	Unternehmensführung (Corporate Governance) und Hauptversammlung 04/2000
Nr. 15	Adolf Wagner	Materialien zur Wachstumsforschung 03/2000
Nr. 16	Thomas Lenk / Anja Birke	Determinanten des kommunalen Gebührenaufkommens unter besonderer Berücksichtigung der neuen Bundesländer 04/2000
Nr. 17	Thomas Lenk	Finanzwirtschaftliche Auswirkungen des Bundesverfassungsgerichtsurteils zum Länderfinanzausgleich vom 11.11.1999 04/2000
Nr. 18	Dirk Bültel	Continous linear utility for preferences on convex sets in normal real vector spaces 05/2000
Nr. 19	Stefan Dierkes / Stephanie Hanrath	Steuerung dezentraler Investitionsentscheidungen bei nutzungsabhängigem und nutzungsunabhängigem Verschleiß des Anlagenvermögens 06/2000
Nr. 20	Thomas Lenk / Andreas Mathes / Olaf Hirschefeld	Zur Trennung von Bundes- und Landeskompetenzen in der Finanzverfassung Deutschlands 07/2000
Nr. 21	Stefan Dierkes	Marktwerte, Kapitalkosten und Betafaktoren bei wertabhängiger Finanzierung 10/2000
Nr. 22	Thomas Lenk	Intergovernmental Fiscal Relationships in Germany: Requirement for New Regulations? 03/2001
Nr. 23	Wolfgang Bernhardt	Stock Options – Aktuelle Fragen Besteuerung, Bewertung, Offenlegung 03/2001
Nr. 24	Thomas Lenk	Die „kleine Reform" des Länderfinanzausgleichs als Nukleus für die „große Finanzverfassungs-reform"? 10/2001

Nr. 25	Wolfgang Bernhardt	Biotechnologie im Spannungsfeld von Menschenwürde, Forschung, Markt und Moral Wirtschaftsethik zwischen Beredsamkeit und Schweigen 11/2001
Nr. 26	Thomas Lenk	Finanzwirtschaftliche Bedeutung der Neuregelung des bundestaatlichen Finanzausgleichs – Eine allkoative und distributive Wirkungsanalyse für das Jahr 2005 11/2001
Nr. 27	Sören Bär	Grundzüge eines Tourismusmarketing, untersucht für den Südraum Leipzig 05/2002
Nr. 28	Wolfgang Bernhardt	Der Deutsche Corporate Governance Kodex: Zuwahl (comply) oder Abwahl (explain)? 06/2002
Nr. 29	Adolf Wagner	Konjunkturtheorie, Globalisierung und Evolutionsökonomik 08/2002
Nr. 30	Adolf Wagner	Zur Profilbildung der Universitäten 08/2002
Nr. 31	Sabine Klinger / Jens Ulrich / Hans-Joachim Rudolph	Konjunktur als Determinante des Erdgasverbrauchs in der ostdeutschen Industrie? 10/2002
Nr. 32	Thomas Lenk / Anja Birke	The Measurement of Expenditure Needs in the Fiscal Equalization at the Local Level Empirical Evidence from German Municipalities 10/2002
Nr. 33	Wolfgang Bernhardt	Die Lust am Fliegen Eine Parabel auf viel Corporate Governance und wenig Unternehmensführung 11/2002
Nr. 34	Udo Hielscher	Wie reich waren die reichsten Amerikaner wirklich? (US-Vermögensbewertungsindex 1800 – 2000) 12/2002
Nr. 35	Uwe Haubold / Michael Nowak	Risikoanalyse für Langfrist-Investments Eine simulationsbasierte Studie 12/2002
Nr. 36	Thomas Lenk	Die Neuregelung des bundesstaatlichen Finanzausgleichs auf Basis der Steuerschätzung Mai 2002 und einer aktualisierten Bevölkerungsstatistik 12/2002
Nr. 37	Uwe Haubold / Michael Nowak	Auswirkungen der Renditeverteilungsannahme auf Anlageentscheidungen Eine simulationsbasierte Studie 02/2003
Nr. 38	Wolfgang Bernhard	Corporate Governance Kodex für den Mittel-Stand? 06/2003
Nr. 39	Hermut Kormann	Familienunternehmen: Grundfragen mit finanzwirtschaftlichen Bezug 10/2003
Nr. 40	Matthias Folk	Launhardtsche Trichter 11/2003
Nr. 41	Wolfgang Bernhardt	Corporate Governance statt Unternehmensführung 11/2003
Nr. 42	Thomas Lenk / Karolina Kaiser	Das Prämienmodell im Länderfinanzausgleich – Anreiz- und Verteilungsmitwirkungen 11/2003
Nr. 43	Sabine Klinger	Die Volkswirtschaftliche Gesamtrechnung des Haushaltsektors in einer Matrix 03/2004
Nr. 44	Thomas Lenk / Heide Köpping	Strategien zur Armutsbekämpfung und –vermeidung in Ostdeutschland: 05/2004
Nr. 45	Wolfgang Bernhardt	Sommernachtsfantasien Corporate Governance im Land der Träume. 07/2004
Nr. 46	Thomas Lenk / Karolina Kaiser	The Premium Model in the German Fiscal Equalization System 12/2004
Nr. 47	Thomas Lenk / Christine Falken	Komparative Analyse ausgewählter Indikatoren des Kommunalwirtschaftlichen Gesamt-ergebnisses 05/2005
Nr. 48	Michael Nowak / Stephan Barth	Immobilienanlagen im Portfolio institutioneller Investoren am Beispiel von Versicherungsunternehmen Auswirkungen auf die Risikosituation 08/2005
Nr. 49	Wolfgang Bernhardt	Familiengesellschaften – Quo Vadis? Vorsicht vor zu viel „Professionalisierung“ und Ver-Fremdung 11/2005
Nr. 50	Christian Milow	Der Griff des Staates nach dem Währungsgold 12/2005

Nr. 51	Anja Eichhorst / Karolina Kaiser	The Instiutional Design of Bailouts and Its Role in Hardening Budget Constraints in Federations 03/2006
Nr. 52	Ullrich Heilemann / Nancy Beck	Die Mühen der Ebene – Regionale Wirtschaftsförderung in Leipzig 1991 bis 2004 08/2006
Nr. 53	Gunther Schnabl	Die Grenzen der monetären Integration in Europa 08/2006
Nr. 54	Hermut Kormann	Gibt es so etwas wie typisch mittelständige Strategien? 11/2006
Nr. 55	Wolfgang Bernhardt	(Miss-)Stimmung, Bestimmung und Mitbestimmung Zwischen Juristentag und Biedenkopf-Kommission 11/2006
Nr. 56	Ullrich Heilemann / Annika Blaschzik	Indicators and the German Business Cycle A Multivariate Perspective on Indicators of Ifo, OECD, and ZEW 01/2007
Nr. 57	Ullrich Heilemann	"The Suol of a new Machine" zu den Anfängen des RWI-Konjunkturmodells 12/2006
Nr. 58	Ullrich Heilemann / Roland Schuhr / Annika Blaschzik	Zur Evolution des deutschen Konjunkturzyklus 1958 bis 2004 Ergebnisse einer dynamischen Diskriminanzanalyse 01/2007
Nr. 59	Christine Falken / Mario Schmidt	Kameralistik versus Doppik Zur Informationsfunktion des alten und neuen Rechnungswesens der Kommunen Teil I: Einführende und Erläuternde Betrachtungen zum Systemwechsel im kommunalen Rechnungswesen 01/2007
Nr. 60	Christine Falken / Mario Schmidt	Kameralistik versus Doppik Zur Informationsfunktion des alten und neuen Rechnungswesens der Kommunen Teil II Bewertung der Informationsfunktion im Vergleich 01/2007
Nr. 61	Udo Hielscher	Monti della citta di firenze Innovative Finanzierungen im Zeitalter Der Medici. Wurzeln der modernen Finanzmärkte 03/2007
Nr. 62	Ullrich Heilemann / Stefan Wappler	Sachsen wächst anders Konjunkturelle, sektorale und regionale Bestimmungsgründe der Entwicklung der Bruttowertschöpfung 1992 bis 2006 07/2007
Nr. 63	Adolf Wagner	Regionalökonomik: Konvergierende oder divergierende Regionalentwicklungen 08/2007
Nr. 64	Ullrich Heilemann / Jens Ulrich	Good bye, Professir Phillips? Zum Wandel der Tariflohndeterminanten in der Bundesrepublik 1952 – 2004 08/2007
Nr. 65	Gunther Schnabl / Franziska Schobert	Monetary Policy Operations of Debtor Central Banks in MENA Countries 10/2007
Nr. 66	Andreas Schäfer / Simone Valente	Habit Formation, Dynastic Altruism, and Population Dynamics 11/2007
Nr. 67	Wolfgang Bernhardt	5 Jahre Deutscher Corporate Governance Kondex Eine Erfolgsgeschichte? 01/2008
Nr. 68	Ullrich Heilemann / Jens Ulrich	Viel Lärm um wenig? Zur Empirie von Lohnformeln in der Bundesrepublik 01/2008
Nr. 69	Christian Groth / Karl-Josef Koch / Thomas M. Steger	When economic growth is less than exponential 02/2008
Nr. 70	Andreas Bohne / Linda Kochmann	Ökonomische Umweltbewertung und endogene Entwicklung peripherer Regionen Synthese einer Methodik und einer Theorie 02/2008
Nr. 71	Andreas Bohne / Linda Kochmann / Jan Slavík / Lenka Slavíková	Deutsch-tschechische Bibliographie Studien der kontingenten Bewertung in Mittel- und Osteuropa 06/2008
Nr. 72	Paul Lehmann / Christoph Schröter-Schlaack	Regulating Land Development with Tradable Permits: What Can We Learn from Air Pollution Control? 08/2008
Nr. 73	Ronald McKinnon / Gunther Schnabl	China's Exchange Rate Impasse and the Weak U.S. Dollar 10/2008
Nr: 74	Wolfgang Bernhardt	Managervergütungen in der Finanz- und Wirtschaftskrise Rückkehr zu (guter) Ordnung, (klugem) Maß und (vernünftigem) Ziel? 12/2008

Nr. 75	Moritz Schularick / Thomas M. Steger	Financial Integration, Investment, and Economic Growth: Evidence From Two Eras of Financial Globalization 12/2008
Nr. 76	Gunther Schnabl / Stephan Freitag	An Asymmetry Matrix in Global Current Accounts 01/2009
Nr. 77	Christina Ziegler	Testing Predictive Ability of Business Cycle Indicators for the Euro Area 01/2009
Nr. 78	Thomas Lenk / Oliver Rottmann / Florian F. Woitek	Public Corporate Governance in Public Enterprises Transparency in the Face of Divergent Positions of Interest 02/2009
Nr. 79	Thomas Steger / Lucas Bretschger	Globalization, the Volatility of Intermediate Goods Prices, and Economic Growth 02/2009
Nr. 80	Marcela Munoz Escobar / Robert Holländer	Institutional Sustainability of Payment for Watershed Ecosystem Services. Enabling conditions of institutional arrangement in watersheds 04/2009
Nr. 81	Robert Holländer / WU Chunyou / DUAN Ning	Sustainable Development of Industrial Parks 07/2009
Nr. 82	Georg Quaas	Realgrößen und Preisindizes im alten und im neuen VGR-System 10/2009
Nr. 83	Ullrich Heilemann / Hagen Findeis	Empirical Determination of Aggregate Demand and Supply Curves: The Example of the RWI Business Cycle Model 12/2009
Nr. 84	Gunther Schnabl / Andreas Hoffmann	The Theory of Optimum Currency Areas and Growth in Emerging Markets 03/2010
Nr. 85	Georg Quaas	Does the macroeconomic policy of the global economy's leader cause the worldwide asymmetry in current accounts? 03/2010
Nr. 86	Volker Grossmann / Thomas M. Steger / Timo Trimborn	Quantifying Optimal Growth Policy 06/2010
Nr. 87	Wolfgang Bernhardt	Corporate Governance Kodex für Familienunternehmen? Eine Widerrede 06/2010
Nr. 88	Philipp Mandel / Bernd Süssmuth	A Re-Examination of the Role of Gender in Determining Digital Piracy Behavior 07/2010
Nr. 89	Philipp Mandel / Bernd Süssmuth	Size Matters. The Relevance and Hicksian Surplus of Agreeable College Class Size 07/2010
Nr. 90	Thomas Kohstall / Bernd Süssmuth	Cyclic Dynamics of Prevention Spending and Occupational Injuries in Germany: 1886-2009 07/2010
Nr. 91	Martina Padmanabhan	Gender and Institutional Analysis. A Feminist Approach to Economic and Social Norms 08/2010
Nr. 92	Gunther Schnabl /Ansgar Belke	Finanzkrise, globale Liquidität und makroökonomischer Exit 09/2010
Nr. 93	Ullrich Heilemann / Roland Schuhr / Heinz Josef Münch	A "perfect storm"? The present crisis and German crisis patterns 12/2010
Nr. 94	Gunther Schnabl / Holger Zemanek	Die Deutsche Wiedervereinigung und die europäische Schuldenkrise im Lichte der Theorie optimaler Währungsräume 06/2011
Nr. 95	Andreas Hoffmann / Gunther Schnabl	Symmetrische Regeln und asymmetrisches Handeln in der Geld- und Finanzpolitik 07/2011
Nr. 96	Andreas Schäfer / Maik T. Schneider	Endogenous Enforcement of Intellectual Property, North-South Trade, and Growth 08/2011
Nr. 97	Volker Grossmann / Thomas M. Steger / Timo Trimborn	Dynamically Optimal R&D Subsidization 08/2011
Nr. 98	Erik Gawel	Political drivers of and barriers to Public-Private Partnerships: The role of political involvement 09/2011
Nr. 99	André Casajus	Collusion, symmetry, and the Banzhaf value 09/2011
Nr. 100	Frank Hüttner / Marco Sunder	Decomposing R^2 with the Owen value 10/2011
Nr. 101	Volker Grossmann / Thomas M. Steger / Timo Trimborn	The Macroeconomics of TANSTAAFL 11/2011

Nr. 102	Andreas Hoffmann	Determinants of Carry Trades in Central and Eastern Europe 11/2011
Nr. 103	Andreas Hoffmann	Did the Fed and ECB react asymmetrically with respect to asset market developments? 01/2012
Nr. 104	Christina Ziegler	Monetary Policy under Alternative Exchange Rate Regimes in Central and Eastern Europe 02/2012
Nr. 105	José Abad / Axel Löffler / Gunther Schnabl / Holger Zemanek	Fiscal Divergence, Current Account and TARGET2 Imbalances in the EMU 03/2012
Nr. 106	Georg Quaas / Robert Köster	Ein Modell für die Wirtschaftszweige der deutschen Volkswirtschaft: Das "MOGBOT" (Model of Germany's Branches of Trade)
Nr. 107	Andreas Schäfer / Thomas Steger	Journey into the Unknown? Economic Consequences of Factor Market Integration under Increasing Returns to Scale 04/2012
Nr. 108	Andreas Hoffmann / Björn Urbansky	Order, Displacements and Recurring Financial Crises 06/2012
Nr. 109	Finn Marten Körner / Holger Zemanek	On the Brink? Intra-euro area imbalances and the sustainability of foreign debt 07/2012
Nr. 110	André Casajus / Frank Hüttner	Nullifying vs. dummifying players or nullified vs. dummified players: The difference between the equal division value and the equal surplus division value 07/2012
Nr. 111	André Casajus	Solidarity and fair taxation in TU games 07/2012
Nr. 112	Georg Quaas	Ein Nelson-Winter-Modell der deutschen Volkswirtschaft 08/2012
Nr. 113	André Casajus / Frank Hüttner	Null players, solidarity, and the egalitarian Shapley values 08/2012
Nr. 114	André Casajus	The Shapley value without efficiency and additivity 11/2012
Nr. 115	Erik Gawel	Neuordnung der W-Besoldung: Ausgestaltung und verfassungsrechtliche Probleme der Konsumtionsregeln zur Anrechnung von Leistungsbezügen 02/2013
Nr. 116	Volker Grossmann / Andreas Schäfer / Thomas M. Steger	Migration, Capital Formation, and House Prices 02/2013
Nr. 117	Volker Grossmann / Thomas M. Steger	Optimal Growth Policy: the Role of Skill Heterogeneity 03/2013
Nr. 118	Guido Heineck / Bernd Süssmuth	A Different Look at Lenin's Legacy: Social Capital and Risk Taking in the Two Germanies 03/2013
Nr. 119	Andreas Hoffmann	The Euro as a Proxy for the Classical Gold Standard? Government Debt Financing and Political Commitment in Historical Perspective 05/2013
Nr. 120	Andreas Hoffmann / Axel Loeffler	Low Interest Rate Policy and the Use of Reserve Requirements in Emerging Markets 05/2013
Nr. 121	Gunther Schnabl	The Global Move into the Zero Interest Rate and High Dept Trap 07/2013
Nr. 122	Axel Loeffler / Gunther Schnabl / Franziska Schobert	Limits of Monetary Policy Autonomy and Exchange Rate Flexibility by East Asian Central Banks 08/2013
Nr. 123	Burkhard Heer / Bernd Süßmuth	Tax Bracket Creep and its Effects on Income Distribution 08/2013
Nr. 124	Hans Fricke / Bernd Süßmuth	Growth and Volatility of Tax Revenues in Latin America 08/2013
Nr. 125	Ulrich Volz	RMB Internationalisation and Currency Co-operation in East Asia 09/2013
Nr. 126	André Casajus / Helfried Labrenz	A property rights based consolidation approach 02/2014
Nr. 127	Pablo Duarte	The Relationship between GDP and the Size of the Informal Economy: Empirical Evidence for Spain 02/2014
Nr. 128	Erik Gawel	Neuordnung der Professorenbesoldung in Sachsen 03/2014
Nr. 129	Friedrun Quaas	Orthodoxer Mainstream und Heterodoxe Alternativen Eine Analyse der ökonomischen Wissenschaftslandschaft 04/2014

Nr. 130	Gene Callahan / Andreas Hoffmann	The Idea of a Social Cycle 05/2014
Nr. 131	Karl Trela	Klimaanpassung als wirtschaftspolitisches Handlungsfeld 06/2014
Nr. 132	Erik Gawel / Miquel Aguado	Neuregelungen der W-Besoldung auf dem verfassungsrechtlichen Prüfstand 08/2014
Nr. 133	Ulf Papenfuß / Matthias Redlich / Lars Steinhauer	Forschend und engagiert lernen im Public Management: Befunde und Gestaltungsanregungen eines Service Learning Lehrforschungsprojektes 10/2014
Nr. 134	Karl Trela	Political climate adaptation decisions in Germany - shortcomings and applications for decision support systems 11/2014
Nr. 135	Ulf Papenfuß / Lars Steinhauer / Benjamin Friedländer	Beteiligungsberichterstattung der öffentlichen Hand im 13-Länder-Vergleich: Erfordernisse für mehr Transparenz über die Governance und Performance öffentlicher Unternehmen 02/2015
Nr. 136	Gunther Schnabl	Japans Lehren für das Schweizer Wechselkursdilemma 02/2015
Nr. 137	Ulf Papenfuß / Christian Schmidt	Determinants of Manager Pay in German State-Owned Enterprises and International Public Policy Implications: 3-Year Study for Sectors, Performance and Gender 02/2015
Nr. 138	Philipp Mandel / Bernd Süßmuth	Public education, accountability, and yardstick competition in a federal system 05/2015
Nr. 139	Gunther Schnabl	Wege zu einer stabilitäts- und wachstumsorientierten Geldpolitik aus österreichischer Perspektive 06/2015
Nr. 140	Ulf Papenfuß / Matthias Redlich / Lars Steinhauer / Benjamin Friedländer	Forschend und engagiert lernen im Public Management: Befunde und Gestaltungsanregungen eines Service Learning Lehrforschungsprojektes – 2. aktualisierte Auflage 08/2015
Nr. 141	Friedrun Quaas / Georg Quaas	Hayeks Überinvestitionstheorie 10/2015
Nr. 142	Bastian Gawellek / Marco Sunder	The German Excellence Initiative and Efficiency Change among Universities, 2001-2011 01/2016
Nr. 143	Benjamin Larin	Bubble-Driven Business Cycles 02/2016
Nr. 144	Friedrun Quaas / Georg Quaas	Effekte des Kapitalmarktzinses auf die Preis- und Produktivitätsentwicklung Eine Analyse der deutschen Volkswirtschaft 1970-2014 02/2016
Nr. 145	Thomas Lenk / Matthias Redlich / Philipp Glinka	Nachhaltige Stadtfinanzen -Akzeptanzsteigerung der bürgerschaftlichen Beteiligung an der Haushaltsplanung 02/2016
Nr. 146	Michael von Prollius / Gunther Schnabl	Geldpolitik, Arabellion, Flüchtlingskrise 10/2016
Nr. 147	David Leuwer / Bernd Süßmuth	The Exchange Rate Susceptibility of European Core Industries, 1995-2010 05/2017
Nr. 148	Gunther Schnabl	Monetary Policy and Wandering Overinvestment Cycles in East Asia and Europe 05/2017
Nr. 149	Ullrich Heilemann / Karsten Müller	Wenig Unterschiede – Zur Treffsicherheit internationaler Prognosen und Prognostiker 07/2017
Nr. 150	Gunther Schnabl / Sebastian Müller	Zur Zukunft der Europäischen Union aus ordnungspolitischer Perspektive 10/2017
Nr. 151	Gunther Schnabl	Ultra-lockere Geldpolitiken, Finanzmarktblasen und marktwirtschaftliche Ordnung 10/2017
Nr. 152	Pablo Duarte / Bernd Süßmuth	Implementing an approximate dynamic factor model to nowcast GDP using sensitivity analysis 02/2018
Nr. 153	Sophia Latsos	Real Wage Effects of Japan's Monetary Policy 03/2018
Nr. 154	Gunther Schnabl / Klaus Siemon	Die EU-Insolvenzrichtlinie zu vorinsolvenzlichen Verfahren aus ordnungspolitischer Perspektive The EU Directive on Preventive Restructuring Frameworks from a Ordoliberal Perspective 07/2018
Nr. 155	Marika Behnert / Thomas Bruckner	Cost effects of energy system stability and flexibility options – an integrated optimal power flow modeling approach 09/2018